Nuclear structure of ^{241}Pu from neutron-capture, (d,p)-, and (d,t)-reaction measurements

D. H. White*
Lawrence Livermore National Laboratory, Livermore, California 94551
and Institut Laue Langevin, 38042 Grenoble, France

R. W. Hoff
Lawrence Livermore National Laboratory, Livermore, California 94551

H. G. Börner, K. Schreckenbach,† F. Hoyler,‡ and G. Colvin§
Institut Laue Langevin, 38042 Grenoble, France

I. Ahmad, A. M. Friedman,‖ and J. R. Erskine¶
Argonne National Laboratory, Argonne, Illinois 60439
(Received 30 September 1997)

We report experimental measurements in ^{241}Pu of the following: primary and secondary γ rays and conversion electrons from thermal neutron capture in ^{240}Pu; γ rays from ^{245}Cm α decay; proton and triton spectra, respectively, from (d,p) and (d,t) reactions on ^{240}Pu and ^{242}Pu targets. From these data and those of other investigations, we have identified 53 excited levels in ^{241}Pu below 1400 keV. Of these, 44 are placed in 10 rotational bands (with connecting transitions) that have been assigned Nilsson configurations. For the bands below 1 MeV in ^{241}Pu that are largely of single-particle character, there is good correspondence with similar bands in ^{239}U and with the theoretical model of Gareev *et al.* For those bands in ^{241}Pu where there is mixing between single-particle and vibrational modes, we find some significant deviations from theoretical predictions. For example, the $\frac{5}{2}[622]\otimes 0^-$ state at 519 keV appears to mix less with other states than predicted, while a trio of $K^\pi=\frac{1}{2}^-$ bands show unexpected mixing patterns. [S0556-2813(98)00503-2]

PACS number(s): 25.40.Lw, 25.45.Hi, 23.20.Lv, 27.90.+b

I. INTRODUCTION

The nuclear level structure associated with an unpaired, 147th neutron is most readily available to the experimentalist in two nuclei, ^{239}U and ^{241}Pu. The former nucleus has been well characterized through neutron-capture γ-ray and transfer-reaction spectroscopy [1,2]. Prior to the present measurements, the level structure of ^{241}Pu was less well known [3], even though a wide variety of experimental techniques had been employed in its measurement. These included spectroscopic determination of γ rays and/or particles emitted during α-decay [4–7], β-decay [8–10], (d,d') inelastic scattering [11], and single-nucleon transfer reactions including (d,p) [11], (d,t) [11,12], and $(^3\mathrm{He},\alpha)$ [12]. The lifetime of the second excited state was studied using the $(d,t\gamma)$ reaction [13]. Previous (n,γ) studies include primary transitions [11,14,15] and secondary transitions [14] following thermal neutron capture, and primary transitions following resonance capture [16].

To obtain the present data, we have used spectrometers of greatly increased resolution and sensitivity for neutron-capture γ-ray [17] and conversion-electron [18] measurements at the Institut-Laue Langevin (ILL) in Grenoble, France. The fission reaction produces serious interferences (via fission-product decay) in the γ spectra from neutron-capture studies of both ^{241}Pu and ^{239}U, although the differing temporal behavior of the fission product and capture γ rays allows one to effectively distinguish between them. Our data have been derived also from measurements of the (d,p) and (d,t) reactions made with improved sensitivity at the Argonne National Laboratory. Inherent advantages in the nuclear spectroscopic study of ^{241}Pu include its population in α decay, β decay, and (d,t) and $(^3\mathrm{He},\alpha)$ reactions, techniques that cannot be applied in the case of ^{239}U.

As compared with previous thermal (n,γ) studies of the levels of ^{241}Pu, the numbers of secondary γ transitions that we have detected (227) and placed in the level scheme (105) are far greater than before where corresponding numbers are (22,22), respectively.[1] Also, our measurements span a much wider range of γ energies, 35–1500 keV, as compared with the rather restricted range previously, 550–840 keV. We have deduced multipolarities from conversion electron measurements for a large fraction (83%) of the observed transi-

*Present address: Western Oregon University, Monmouth, OR 97361.
†Present address: Technical University of Munich, D-85748 Garching, Germany.
‡Present address: University of Tübingen, D-72076 Tübingen, Germany.
§Present address: Harwell Laboratory, OX 11 ORA, Great Britain.
‖Deceased.
¶Present address: Office of Energy Research, U.S. Department of Energy, Germantown, MD 20874-1290.

[1]Apparently, the authors have reported only those gamma transitions that they were able to place in their level scheme [14].

tions (previously 15%). We have measured energies and intensities for 30 primary γ rays (3600–5100 keV), as compared to 17 that were measured previously.

We report new experimental data from (d,p)- and (d,t)-reaction measurements at the Argonne National Laboratory in Illinois that supplement existing data by identifying nine levels not previously observed in these spectra.

II. EXPERIMENTAL METHODS

A. Secondary gamma rays from thermal neutron capture

Secondary γ rays following thermal neutron capture in ^{240}Pu ($\sigma_\gamma = 291$b) were measured using the curved-crystal spectrometers GAMS1 and GAMS2/3 at the Institut Laue-Langevin (ILL) in Grenoble. Two targets were used, each consisting of about 4 mg of $^{240}PuO_2$ (enriched to 99.46%) in the form of a wafer of height 4.65 cm and width 0.57 cm. The GAMS spectrometers are situated on opposite sides of a horizontal beam tube, and view the target situated in a thermal neutron flux of 5.5×10^{14} neutrons/cm^2 s. The GAMS1 spectrometer was used to measure the γ rays in the range 35–500 keV; the energy resolution (FWHM in eV) was $5.6\times10^{-6}E_\gamma^2(keV)/n$, where n is the order of diffraction. The GAMS2/3 spectrometer was used to span the range 150–1500 keV; the energy resolution (FWHM in eV) was $2.0\times10^{-6}E_\gamma^2(keV)/n$. The method of analysis of these data has been described in detail previously [17].

Since ^{241}Pu has a thermal neutron fission cross section of 1010 b, which is significantly larger than the cross section for its production in a ^{240}Pu target, irradiation in a high neutron flux will produce a rapid growth of fission-product γ rays. These γ rays, along with those from second-order neutron capture, produce an intense, ever-growing background of discrete lines and, thus, represent a serious interference with the observation of γ rays from the de-excitation of ^{241}Pu nuclei. In order to most effectively identify spectral lines that were increasing temporally, two separate irradiations were made, each starting with a new target and each lasting about one week. During each run, the ^{240}Pu in the target decreased by about 10%, whereas the ^{241}Pu content of the target increased almost linearly. The first run was taken in the direction of increasing angle of diffraction (decreasing energy), and the second in the direction of decreasing angle of diffraction. Since the two runs were scanned in opposite directions, and since the spectra were observed in five orders of diffraction, the various energy regions were observed at several different times of irradiation. Therefore, in almost all cases, we were able to distinguish between peaks that were growing and those that were not. The former, constituting the majority, were deleted from the compilation.

Energy calibration of the measured γ rays was performed by making a best fit to the reported values of the plutonium $K\alpha_1$ and $K\alpha_2$ energies, 103.741 ± 0.002 and 99.521 ± 0.002 keV, respectively [20]. Intensity calibrations were carried out by folding the measured intensities, corrected for burnup, with previously determined instrumental efficiencies, and corrected for self-absorption by a comparison of γ-ray data with the corresponding electron intensities of known multipolarity. Absolute intensities were determined by assuming that we observe about 95% of the total transition strength populating the ground state.

The complete set of γ-ray energies and intensities attributed to ^{241}Pu is given in Table I. Values of energy and relative intensity were assigned a figure of merit (A–D; see column 3 in Table I). The γ-ray energies in the present data set are much more precise than those reported previously for transitions in ^{241}Pu, e.g., the average uncertainty for the 33 transitions in Table I with $E_\gamma<200$ keV is 2.5 eV compared with an average of 60 eV for 12 transitions, previously. Similarly, for transitions with $E_\gamma>300$ keV, the average uncertainty for transitions in Table I is 7.6 eV compared with an average of 200 eV previously. This improved precision has been of considerable benefit in constructing the level scheme since it has allowed for much greater certainty in the placement of transitions using the Ritz combination technique.

B. Conversion electrons from thermal neutron capture

The conversion electrons following thermal neutron capture in ^{240}Pu were studied with the BILL electron spectrometer at the ILL [18]. Two targets were employed: a thin target (46 μg/cm^2) was used in the range 18–100 keV, and a thicker target (298 μg/cm^2) in the range 100–1500 keV. The thermal neutron flux at the in-pile target position was 3×10^{14} neutrons cm^{-2} s^{-1}. The momentum resolution obtained was $\Delta p/p=5\times10^{-4}$. Relative intensities and energies were aligned in the overlap region and were corrected for self-absorption at low energies by a comparison of subshell ratios of known transitions. The resulting intensities and energies were calibrated against the γ rays using transitions of known multipolarity (usually $E1$ or pure $E2$). Multipolarities of strong transitions were determined from L-subshell ratios and those of weaker transitions from absolute conversion coefficients [19]. In cases of weak transitions, the absence of conversion electron peaks set an upper limit on the conversion coefficient, resulting in partial information of the multipolarity (e.g., limiting the transition to $E1$ or $E2$). Several low-energy transitions were identified by the conversion electrons even though no γ-rays were detected. The measured conversion electron energies, conversion coefficients, and deduced multipolarities are listed in Table II together with the corresponding γ rays. The detection of multiple conversion electron lines, as is the case for transitions listed in Table II, allows one to place greater confidence (indicated in column 3 of Table 1) in their origin, namely ^{241}Pu decay.

C. Primary gamma-rays from thermal neutron capture

Primary γ rays following thermal neutron capture were measured with a three-crystal pair spectrometer located downstream of the GAMS1 spectrometer at ILL. The pair spectrometer [21] consists of a Ge(Li) detector, flanked by two NaI(Tl) detectors for coincidence detection of 511 keV annihilation quanta. Several spectra were taken and combined. The resulting spectrum was analyzed for peaks in the interval 3600–5100 keV. Aluminum and carbon, present in the source assembly, provided precisely known peaks [22] for energy calibration of the spectrum. Although the Al peaks strongly dominated the spectrum, the Pu/Al ratio in the two targets used was different, which allowed a means of

TABLE I. Secondary γ rays from thermal-neutron capture in ^{240}Pu.

Energy [a] (keV)	Intensity [b] (per 100 n)	Conf. [c]	Elec. shell	α_{exp} [d]	Multi-polarity [e]	Lvl. energies [f] $E_{init}-E_{final}$
35.788(1)	0.100(12)	D				
41.972(1) [g]	0.146(5)	A	L_I	53(8)	$M1e2$	42–0
51.325(2)	0.049(5)	C				
52.048(2)	0.054(6)	A	L_{II}	33(6)	$M1E2$	223–171
53.807(1) [g]	0.086(11)	A	L_I	17(3)	$M1e2$	96–42
56.89(3) [h]	0.33(3)[i]	B				232–175
57.806(2)	0.066(10)	B			$E1$?	842–784
61.303(1)	0.091(3)	B	L_{II}	66(10)	$E2$	223–162
62.812(2)	0.067(5)	D				
65.535(3)	0.164(7)	C	L_I	14.0(21)	$M1$	161–96
68.904(2)	0.029(5)	B	L_I	11.8(25)	$M1$	869–800($\frac{5}{2}$)
71.390(2)	0.042(3)	B	L_I	10.0(25)	$M1e2$	851–779
72.584(3)	0.018(3)	D				
73.950(1)	0.056(3)	B	L_{II}	21(3)	$E2$	245–171
75.331(2)	0.034(6)	D				
79.262(7)	0.007(2)	C	L_I	5.8(10)	$M1E2$	175–96
86.783(1)	0.134(6)	B			$E1$?	842–755
86.965(4)	0.023(4)	C				
95.365(1)	0.077(4)	B			$E1$?	851–755
95.786(3)	0.013(2)	B	L_{II}	7.6(12)	$E2$	96–0
114.148(2)	0.097(5)	A	L_{II}	3.1(5)	$E2$	337–223
119.734(5)	0.032(4)	C				
126.09(4) [h]	0.07(2)[i]	B				301–175
133.081(2) [g]	01.11(3)	A	L_I	1.9(3)	$M1e2$	175–42
136.127(20) [g,j]	0.029(5)	B	L_I	1.22(21)	$M1E2$	232–96
139.87(4) [h]	0.09(1)[i]	B				301–161
149.107(6)	0.035(5)	B	K	6.5(13)	$M1$	245–96
161.685(1) [g]	20.57 (20)	A	L_{II}	0.71(11)	$E2$	162–0
170.940(1)	0.378(7)	A	K	4.9(7)	$M1$	171–0
175.051(2) [g]	0.362(4)	A	K	3.7(6)	$M1e2$	175–0
181.017(2)	0.250(7)	A	K	3.8(6)	$M1e2$	223–42
185.132(22)	0.004(2)	D	K	0.08(3)	$E1$	940–755
187.414(6)	0.042(9)	C	K	1.9(5)	$M1E2$	943–755
189.965(10) [g]	0.020(2)	B	K	2.9(5)	$M1E2$	232–42
195.669(10)	0.038(5)	C	K	3.4(6)	$M1$	965–769
202.910(7)	0.039(7)	B	L_I	0.34(7)	$M1E2$	245–42
205.404(20) [h]	0.08(1)[i]	B				301–96
209.745(9)	0.037(9)	C	K	0.40(16)	$E1E2$	965–755
211.666(11)	0.063(18)	C				
222.971(3)	0.126(5)	A	K	1.9(4)	$M1E2$	223–0
229.403(4)	0.095(6)	A	K	0.130(22)	$E2$	404–174
231.96(3) [h]	0.11(2)[i]	B				232–0
233.844(3)	0.121(4)	A			$E1$?	409–175
239.493(8)	0.055(5)	B	K	2.0(3)	$M1$	1090–851
240.167(12)	0.040(5)	C	K	2.1(4)	$M1$	1009–769
240.986(7)	0.054(4)	C	K	0.23(4)	$E2m1$	
241.381(17)	0.052(6)	D	K	0.53(10)	$E2m1$	337–96
247.129(23)	0.063(8)	C	K	0.20(4)	$M1E2$	
247.591(4)	0.099(9)	A				
248.066(6)	0.076(6)	A	K	1.50(25)	$M1e2$	1090–842
277.992(9)	0.062(16)	C				
278.420(20)	0.053(5)	B				
308.674(2)	0.503(8)	A	K	0.033(5)	$E1$	404–96

TABLE I. (*Continued*).

Energy [a] (keV)	Intensity [b] (per 100 n)	Conf. [c]	Elec. shell	α_{exp} [d]	Multi-polarity [e]	Lvl. energies [f] $E_{init}-E_{final}$
313.123(4)	0.110(7)	B			$E1$?	409–96
320.746(7)	0.056(4)	B	K	0.84(14)	$M1$	1090–769
359.149(13)	0.045(11)	D	K	0.060(17)	$E2$	534–175
362.479(2)	1.271(18)	A	K	0.024(4)	$E1$	404–42
367.101(76)	0.370(13)	B			$E1$?	409–42
382.164(15)	0.047(5)	C				
388.16(5) [h]	0.19(1)[i]	B				
402.540(30)	0.101(23)	C	K	0.017(5)	$E1$	
403.260(14)	0.061(9)	D	K	0.090(18)	$E2m1$	1254–851
404.707(10)	0.056(8)	C				
405.899(50)	0.056(12)	D	K	0.050(14)	$E2$	
408.699(31)	0.048(7)	D	K	0.30(9)	$M1E2$	
429.139(22)	0.040(6)	D	K	0.090(20)	$E2m1$	
439.382(20)	0.066(7)	C	K	0.063(13)	$E2m1$	
439.750(6)	0.117(7)	B	K	0.025(5)	$E1$	
444.687(9)	0.126(18)	D	K	0.013(3)	$E1$	1224–779
464.775(57)	0.063(13)	D	K	0.020(6)	$E1$	
465.646(5)	0.287(11)	B	K	0.019(3)	$E1$	561–96
468.233(50)	0.071(15)	D	K	0.060(15)	$E2m1$	
476.840(3)	1.044(46)	A	K	0.020(3)	$E1E2$	519–42
483.662(6)	0.528(67)	A				
484.521(7)	0.422(20)	A	K	0.0130(21)	$E1$	1254–769
490.624(9)	0.184(14)	B	K	0.24(4)	$M1e2$	1009–519
490.927(8)	0.195(16)	B				
491.423(10)	0.409(23)	A	K	0.026(4)	$E1E2$	
496.217(4)	0.489(9)	A	K	0.0140(22)	$*E1$	833–337
496.217(4)	0.489(9)	A	K	0.0140(22)	$*E1$	1297–800($\frac{3}{2}$)
501.447(28)	0.121(14)	B	K	0.012(3)	$E1$	
513.504(9)	0.177(17)	B			$E1$?	
515.701(32)	0.101(20)	C	K	0.13(4)	$E2M1$	1358–842
515.952(31)	0.103(19)	C	K	0.063(13)	$E2m1$	
518.810(4)	3.213(58)	A	K	0.0120(18)	$E1$	519–0
519.433(8)	0.528(36)	A	K	0.040(21)	$E1E2$	561–42
520.505(23)	0.094(13)	D				
521.106(27)	0.073(13)	D	K	0.054(13)	$E2m1$	
527.258(25)	0.064(18)	C	K	0.080(26)	$E2M1$	
528.199(44)	0.079(9)	C	K	0.35(7)	$E0M1$	
541.594(6)	0.435(34)	A	K	0.0130(22)	$E1$	
546.479(25)	0.081(10)	C	K	0.014(4)	$E1$	
549.115(9)	0.244(11)	B				
556.164(3)	2.948(47)	A	K	0.0099(15)	$E1$	779–223
561.168(4)	2.248(51)	A	K	0.160(24)	$M1e2$	784–223
561.437(20)	0.365(19)	B	K	0.038(8)	$E2m1$	561–0
566.057(4)	1.168(44)	A	K	0.0090(13)	$E1$	811–245
572.863(9)	0.134(12)	A	K	0.022(6)	$E1$	615–42
575.084(20)	0.200(18)	B	K	0.068(12)	$E2M1$	
576.681(84)	0.045(12)	C	K	0.19(6)	$M1$	
577.561(4)	1.138(33)	A	K	0.130(21)	$M1E2$	
584.431(12)	0.191(25)	B				
586.703(16)	0.097(10)	B	K	0.18(3)	$M1$	832–245
587.953(24)	0.099(10)	C				811–223
593.488(4)	2.695(37)	A	K	0.140(21)	$M1e2$	755–162
598.328(6)	2.512(39)	A	K	0.0084(12)	$E1$	769–171
598.830(24)	0.133(15)	D	K	0.080(15)	$E2M1$	

TABLE I. (*Continued*).

Energy [a] (keV)	Intensity [b] (per 100 n)	Conf. [c]	Elec. shell	α_{exp} [d]	Multi-polarity [e]	Lvl. energies [f] $E_{init}-E_{final}$
602.530(30)	0.225(45)	C	*K*	0.13(3)	*M*1*E*2	1358–755
605.546(7)	0.518(11)	A	*K*	0.0130(22)	*E*1	
607.580(5)	1.570(38)	A	*K*	0.0090(13)	*E*1	769–162
608.229(9)	0.437(16)	B			*E*1?	779–171
608.608(10)	0.379(12)	B	*K*	0.120(19)	*M*1*E*2	832–223
617.457(5)	2.171(33)	A	*K*	0.0100(25)	*E*1	779–162
618.950(82)	0.051(13)	D				
622.464(14)	0.190(12)	B	*K*	0.119(19)	*M*1*E*2	784–162
624.015(39)	0.079(10)	C	*K*	0.106(20)	*M*1*E*2	
627.552(5)	1.335(25)	A	*K*	0.0110(17)	*E*1	851–223
629.539(6)	1.492(30)	A	*K*	0.107(16)	*M*1*E*2	800($\frac{5}{2}$)–171
634.193(23)	0.172(8)	B	*K*	0.098(15)	*M*1*E*2	
638.757(5)	1.079(25)	A	*K*	0.097(15)	*M*1*E*2	800($\frac{3}{2}$)–162
640.001(6)	1.103(37)	A	*K*	0.0080(13)	*E*1	811–171
642.25(3)	0.067(23)	C	*K*	0.11(4)	*M*1*E*2	
652.38(8)	0.111(11)	C	*K*	0.019(4)	*E*2	
656.035(23)	0.141(13)	D	*K*	0.040(7)	*E*2*M*1	
660.625(13)	0.593(28)	A	*K*	0.096(15)	*M*1*E*2	832–171
663.374(31)	0.077(71)	D	*K*	0.030(3)	*E*2*m*1	
671.007(9)	0.303(14)	B	*K*	0.0080(15)	*E*1	842–171
680.274(16)	0.376(10)	B	*K*	0.011(4)	*E*1	842–162
688.851(14)	0.678(24)	A	*K*	0.0060(10)	*E*1	851–162
698.661(24)	0.143(8)	B	*K*	0.025(4)	*E*2	
704.70(14)	0.093(25)	C	*K*	0.016(5)	*E*2	800($\frac{5}{2}$)–96
708.01(6)	0.138(23)	C	*K*	0.050(11)	*E*2*M*1	869–161
726.562(22)	0.180(8)	B	*K*	0.017(3)	*E*2	898–171
737.922(20)	0.219(14)	B	*K*	0.070(13)	*M*1*E*2	
742.250(9)	1.088(42)	A	*K*	0.049(8)	*E*2*M*1	
749.67(5)	0.240(25)	C	*K*	0.016(4)	*E*2	
750.19(4)	0.313(33)	C	*K*	0.053(10)	*M*1*E*2	
751.16(6)	0.125(22)	C	*K*	0.022(5)	*E*2	
751.92(6)	0.126(22)	C	*K*	0.055(12)	*M*1*E*2	
755.154(14)	0.580(45)	A	*K*	0.018(3)	*E*2	755–0
758.494(15)	0.377(23)	A	*K*	0.0080(16)	**E*1*E*2	800($\frac{3}{2}$)–42
758.494(15)	0.377(23)	A	*K*	0.0080(16)	**E*1*E*2	800($\frac{5}{2}$)–42
760.13(8)	0.084(21)	C	*K*	0.11(3)	*E*0*M*1	
765.23(3)	0.212(16)	B	*K*	0.0090(19)	*E*2	940–175
771.64(4)	0.162(83)	C	*K*	0.035(19)	*E*2*M*1	943–171
772.645(21)	0.488(45)	B	*K*	0.0030(6)	*E*1	996–223
773.59(4)	0.197(21)	B	*K*	0.040(8)	*E*2*M*1	869–96
777.89(5)	0.132(13)	C	*K*	0.050(9)	*M*1*E*2	1297–519
780.889(8)	1.904(32)	A	*K*	0.061(9)	*M*1*E*2	943–162
784.153(16)	0.518(16)	A	*K*	0.017(3)	*E*2	784–0
786.454(16)	0.49(3)	C				1009–223
789.63(4)	0.218(23)	B	*K*	0.059(11)	*M*1*E*2	832–42
793.95(5)	1.082(83)	B				965–171
794.27(5)	1.126(81)	B	*K*	0.049(8)	*M*1*E*2	
800.461(11)	0.742(25)	A	*K*	0.044(7)	**M*1*E*2	800($\frac{3}{2}$)–0
800.461(11)	0.742(25)	A	*K*	0.044(7)	**M*1*E*2	800($\frac{5}{2}$)–0
803.265(19)	0.583(16)	A	*K*	0.0039(6)	*E*1	965–162
811.982(19)	0.480(23)	B	*K*	0.035(6)	*E*2*M*1	
833.904(13)	0.807(28)	B	*K*	0.0050(9)	*E*1	996–162

TABLE I. (*Continued*).

Energy [a] (keV)	Intensity [b] (per 100 n)	Conf. [c]	Elec. shell	α_{exp} [d]	Multi-polarity [e]	Lvl. energies [f] $E_{init}-E_{final}$
834.837(17)	0.512(26)	B	*K*	0.040(6)	*M*1*E*2	835–0
838.646(22)	0.449(24)	B	*K*	0.0150(26)	*E*2	
844.200(20)	0.306(48)	C	*K*	0.028(6)	*E*2*M*1	
845.07(5)	0.215(23)	C	*K*	0.0040(11)	*E*1	
848.12(6)	0.172(22)	C				
853.31(6)	0.106(12)	C	*K*	0.033(7)	*E*2*M*1	
876.58 (10)	0.282(94)	C	*K*	0.008(3)	*E*1*E*2	
892.934(18)	0.419(21)	A	*K*	0.058(9)	*M*1	
931.667(20)	0.741(38)	B	*K*	0.028(4)	*E*2*M*1	
940.315(12)	2.211(84)	B	*K*	0.027(4)	*E*2*M*1	940–0
941.12(3)	1.228(53)	D	*K*	0.0090(14)	*E*2	
942.58(4)	0.492(55)	D	*K*	0.0040(8)	*E*1	943–0
953.20(4)	0.728(46)	B	*K*	0.0100(21)	*E*2	
958.30(11)	0.169(33)	C	*K*	0.0080(24)	*E*2	
965.07(12)	0.147(36)	D				
967.46(13)	0.191(34)	D				
973.70(10)	0.55(11)	B	*K*	0.013(3)	*E*2*m*1	
999.37(15)	0.175(24)	C	*K*	0.58(12)	*E*0*M*1	
100.325(9)	0.338(31)	C	*K*	0.0100(18)	*E*2	
100.621(13)	0.47(15)	C	*K*	0.0040(14)	*E*1	
100.695(12)	0.57(15)	C			*E*1?	
100.930(10)	0.31(11)	C			*E*1?	
102.039(6)	0.281(63)	C	*K*	0.0070(19)	*E*2*E*1	
102.295(7)	0.280(35)	C	*K*	0.0100(21)	*E*2	
102.598(7)	0.288(36)	C	*K*	0.0040(12)	*E*1	
103.475(18)	0.263(32)	B	*K*	0.0040(10)	*E*1	
103.726(10)	0.268(42)	C			*E*1?	
103.989(13)	0.191(40)	C	*K*	0.031(8)	*M*1*E*2	
104.500(6)	0.362(66)	B	*K*	0.0060(15)	*E*2*E*1	
1052.927(28)	0.824(38)	A	*K*	0.0026(4)	*E*1	1224–171
1060.64(15)	0.206(36)	C	*K*	0.0060(15)	*E*2*E*1	
1062.31(4)	0.81(11)	B	*K*	0.0031(6)	*E*1	
1064.28(11)	0.211(33)	C	*K*	0.022(5)	*M*1*E*2	
1073.00(10)	0.376(50)	C	*K*	0.0060(14)	*E*2*E*1	
1074.44(11)	0.455(50)	C				
1078.15(7)	0.325(67)	B				
1082.80(4)	0.623(34)	A	*K*	0.0025(4)	*E*1	1254–171
1089.94(4)	1.061(82)	A	*K*	0.0025(4)	*E*1	
1092.08(5)	0.885(54)	A	*K*	0.0030(5)	*E*1	1254–162
1134.445(76)	0.527(35)	B	*K*	0.0029(8)	*E*1	
1146.493(78)	0.444(34)	B	*K*	0.0056(10)	*E*1*E*2	
1155.258(95)	0.388(31)	B	*K*	0.0039(8)	*E*1*E*2	
1170.019(56)	0.632(37)	B	*K*	0.0105(16)	*M*1*E*2	
1174.00(15)	0.232(42)	C				
1177.835(98)	0.395(33)	C				
1180.637(71)	0.598(60)	B	*K*	0.0097(17)	*M*1*E*2	
1196.31(20)	0.600(52)	C	*K*	0.0037(7)	*E*1*E*2	
1200.87(11)	0.419(48)	C	*K*	0.0120(23)	*M*1*E*2	
1203.343(77)	0.539(48)	C	*K*	0.0035(6)	*E*1	
1206.573(51)	1.342(69)	B	*K*	0.0103(16)	*M*1	
1214.65(12)	0.478(35)	C	*K*	0.0039(7)	*E*1*E*2	
1228.02(19)	0.357(67)	D	*K*	0.0039(10)	*E*1*E*2	
1235.282(80)	0.573(51)	C	*K*	0.0100(19)	*M*1*E*2	
1255.32(11)	0.637(42)	C	*K*	0.020(3)	*M*1*E*2	

TABLE I. (*Continued*).

Energy [a] (keV)	Intensity [b] (per 100 n)	Conf. [c]	Elec. shell	α_{exp} [d]	Multi-polarity [e]	Lvl. energies [f] $E_{init}-E_{final}$
1266.14(11)	0.604(70)	B	*K*	0.0022(4)	*E*1	
1267.951(95)	0.85(11)	B	*K*	0.0031(6)	*E*1	
1276.7(12)	0.57(10)	D				
1301.0(14)	0.489(90)	C				
1303.46(34)	0.303(53)	C	*K*	0.0032(9)	*E*1*E*2	
1315.594(54)	0.956(43)	B	*K*	0.0040(6)	*E*1*E*2	
1332.30(15)	0.852(82)	C	*K*	0.0017(3)	*E*1	
1352.64(10)	0.63(14)	B	*K*	0.0076(20)	*M*1*E*2	
1378.52(22)	0.265(36)	D	*K*	0.0060(14)	*E*2*M*1	
1393.494(98)	0.774(45)	B	*K*	0.0140(22)	*M*1*E*2	
1423.89(20)	0.59(11)	D				
1491.35(11)	0.80(13)	B	*K*	0.0090(19)	*M*1*E*2	
1502.84(28)	0.483(95)	C	*K*	0.0028(7)	*E*1*E*2	
1512.38(13)	0.704(66)	B	*K*	0.0014(3)	*E*1	

[a]The γ-rays were measured with the GAMS1 and GAMS2/3 spectrometers, unless otherwise noted; see footnote h. Uncertainties in the last digits are given in parentheses.

[b]Listed are absolute γ-ray intensities obtained from the total intensity populating the ground state.

[c]Indication of confidence for transitions. A: well established; B: probable; C: possible; D: tentative.

[d]Listed are experimental conversion coefficients for the specific electron shells given in the preceding column.

[e]Multipolarities have been deduced from conversion coefficient data. $M1E2$ denotes a mixture with $>50\%$ $M1$ character and $>20\%$ $E2$ character; $M1e2$ denotes a mixture with $<20\%$ $E2$ character, etc. $E1E2$ indicates an experimental conversion coefficient that does not permit choosing between these alternatives. $E1?$ indicates a transition where no conversion electrons have been detected and the photon intensity is sufficiently great to allow the deduction of $E1$ character. An asterisk denotes multiple placement of the transition in the decay scheme.

[f]Listed are level energies (in keV) of the initial and final states connected by the transition whose energy is given in column 1.

[g]γ ray also detected in ^{245}Cm α-decay γ spectrum.

[h]γ ray observed only in ^{245}Cm α-decay γ spectrum.

[i]The listed intensity for this photon is given relative to $I_{175}=100$ (arbitrary units) in ^{245}Cm α decay.

[j]The intensity of this 136.127-keV photon in the (n,γ) spectrum is too large, relative to that of the 189.965-keV line, as compared with their relative intensities measured in the ^{245}Cm α decay. Apparently this discrepancy is due to interference from a fission-product γ ray. The energy of the 136-keV transition has been derived from conversion-electron data.

directly identifying ^{241}Pu peaks. The γ rays attributed to primary transitions following thermal neutron capture are listed in Table III.

D. Gamma rays from ^{245}Cm α decay

A 0.3-mg sample of isotopically pure ^{245}Cm (that was chemically separated from a large quantity of ^{249}Cf) was used as a source in the measurement of its α-decay γ rays. A conventional Ge(Li) detector and pulse-height analyzer (pha) combination was used to record the spectrum. Six low-energy γ rays that had also been detected in the thermal neutron (n,γ) spectrum (those labeled with a superscript g in Table I) served to calibrate the Ge(Li)-pha system. Several additional γ rays were detected in the ^{245}Cm spectrum and are also listed in Table I (see those entries labeled with h and i). We do not find evidence for γ rays with energies 165.3, 185.8, and 210.6 keV that were reported previously [6].

E. (d,p) and (d,t) reaction measurements

Previously, Braid *et al.* [11] studied ^{241}Pu level structure by means of neutron transfer reactions. Their data show a concentration of levels in the 700–1000 keV region. In order to better resolve the peaks in this region and to obtain more precise energies and cross sections for these levels, we have repeated the measurements with higher resolution than before. Thin targets of ^{240}Pu and ^{242}Pu were prepared with an electromagnetic isotope separator on 40 μg/cm^2 carbon backing. These targets were bombarded with 12.0-MeV deuteron beams from the Argonne FN tandem Van de Graaff accelerator. The emitted protons and tritons were momentum analyzed with an Enge split-pole magnetic spectrometer. Emulsion plates placed at the focal plane of the spectrometer served to detect the charged particles. Both the proton and triton spectra had resolution [full width at half maximum (FWHM)] of 7.0 keV. The (d,p) and (d,t) spectra were measured at 90°, 120°, and 150°. Strong peaks were observed at all angles but the proton spectrum at 90° and the

TABLE II. Conversion-electron subshell intensity ratios for transitions in ^{241}Pu. For a given transition, the entries on the first line are experimental values with uncertainties on the last digits given in parentheses and the entries on the second line are theoretical values for the multipolarity mixture given in the last column.

E_γ	L_I/K	L_I	L_{II}	L_{III}	M_I/L_I [a]	M_I	M_{II}	M_{III}	Multipolarity [b]
41.972		100	40(2)	26(1)	0.23(1)	100	45(2)	26(1)	
		100	41	26	0.24	100	45	31	$M1+4\%E2$
52.048		100	140(6)	104(4)	0.23(1)	100	151(6)	131(6)	
		100	138	106	0.24	100	153	122	$M1+21\%E2$
53.807		100	30(1)	18.1(5)	0.21(1)				
		100	30	16.6	0.24				$M1+4\%E2$
61.303		4.7(2)	100	76(3)	0.26(1) M_{II}/L_{II}		100	81(3)	
		3.9	100	79	0.27		100	81	$E2$
68.904		100	15.7(16)		0.26(1)	100	29(4)		
		100	15.7		0.24	100	17		$M1+1.5\%E2$
71.390					0.21(1)	100	17.5(28)		
					0.24	100	17.5		$M1+20\%E2$
73.950			100	76(7)	0.27(2) M_{II}/L_{II}		100	76(7)	
			100	76	0.27		100	76	$E2$
95.786			100	74(3)	0.17(1) M_{II}/L_{II}				
			100	67	0.28				$E2$
114.148		6.8(6)	100	68(2)	0.33(1) M_{II}/L_{II}				
		6.2	100	62	0.29				$E2$
133.081		100	18.4(5)	21.6(6)	0.22(1)	100	19.5(12)		
		100	17.8	24.1	0.24	100	19.9		$M1+6\%E2$
149.107		100	11.5(3)						
		100	11.5						$M1+0.4\%E2$
161.685	0.36(1)	10.0(3)	100	58(2)	0.30(1) M_{II}/L_{II}	12.4(6)	100	57(2)	
	0.43	10.0	100	53	0.27	10.7	100	56	$E2$
170.940	0.18(1)	100	10.6(3)		0.22(1)	100	13.0(6)		
	0.18	100	11.2		0.24	100	12.5		$M1$
175.051	0.18(1)	100	16.4(6)		0.25(1)				
	0.18	100	16.4		0.24				$M1+7\%E2$
181.017	0.18(1)	100	15.6(10)		0.24(1)	100	12.2(14)		
	0.18	100	15.6		0.24	100	17.4		$M1+6\%E2$
189.965	0.15(1)	100	38(5)		0.24(7)				
	0.18	100	38		0.24				$M1+31\%E2$
202.911	0.10(1)	100	38(2)		0.21(2)				
	0.18	100	38		0.24				$M1+34\%E2$
222.971	0.17(1)	100	31(2)	9.1(8)	0.20(4) M_{II}/L_{II}		100	110(24)	
	0.18	100	31	9.5	0.24		100	32	$M1+30\%E2$
248.066	0.17(1)	100	16.7(12)		0.23(1)				
	0.18	100	16.7		0.24				$M1+12\%E2$

[a]The subshell ratios listed in this column are M_I/L_I unless an entry follows the ratio indicating otherwise.
[b]It is understood that the percentage mix for the two components listed, e.g., $M1+4\%E2$, sums to 100%.

triton spectrum at 150° provided the best results. The level energies, averaged from all spectra, and proton cross sections at 90° and triton cross sections at 150° are listed in Table IV. Only statistical uncertainties are given in the table. The uncertainties of the absolute cross sections are estimated to be ~20%. Ratios of cross sections at 90° and 150° provided information about the ℓ transfer in the reactions. These were found to be consistent with the assignments made from the (n,γ) data. The ratio of (d,p) cross section to that of the (d,t) cross section provided information on the particle or hole character of the state being populated. The results of the present work are in good agreement with previous measurements. In the (d,p) spectrum, weakly populated states at 1220, 1257, 1275, 1288, 1297, 1308, 1356, 1450, 1495, 1742, and 1805 keV were observed at 120° and 150°. Levels at these energies have also been reported by Braid *et al.*

TABLE III. Primary γ rays from thermal neutron capture in ^{240}Pu.

E_γ[a] (keV)	$E_{\rm lvl}$ (keV)	I_γ (rel)[b]	E_γ[a] (keV)	$E_{\rm lvl}$ (keV)	I_γ (rel)[b]
5079.80(2)	161.72(2)	2.76(14)	3987.74(2)	1253.80(2)	6.4(3)
5071.8(10)	169.7(10)	0.58(24)	3972.68(5)	1268.86(3)	0.54(3)
4486.19(19)	755.34(19)	0.48(5)	3944.81(4)	1296.73(2)	12.7(7)
4472.29(4)	769.24(4)	3.7(3)	3925.30(10)	1316.24(10)	0.90(6)
4457.42(3)	784.11(3)	2.34(13)	3889.94(20)	1351.60(20)	1.9(4)
4441.12(9)	800.41(9)	0.53(3)	3883.89(4)	1357.65(2)	13.0(7)
4399.54(10)	841.99(10)	2.12(15)	3878.71(8)	1362.83(8)	2.12(14)
4390.97(3)	850.56(3)	5.42(4)	3769.46(12)	1472.08(12)	0.58(12)
4301.25(5)	940.28(5)	2.7(3)	3763.36(13)	1478.18(13)	0.58(5)
4298.95(6)	942.58(6)	2.50(28)	3740.22(21)	1501.32(21)	0.64(8)
4276.61(2)	964.92(2)	6.1(3)	3736.33(19)	1505.21(19)	0.74(8)
4245.84(4)	995.69(4)	2.39(14)	3727.57(10)	1513.97(10)	1.49(11)
4232.04(5)	1009.49(5)	1.65(10)	3717.81(5)	1523.73(4)	4.67(27)
4151.53(2)	1090.00(2)	6.6(3)	3710.63(20)	1530.91(20)	1.9(5)
4017.80(6)	1223.74(6)	3.19(23)	3630.52(3)	1611.02(3)	2.4(6)

[a]Energy not corrected for recoil.

[b]Relative intensities are given in arbitrary units.

III. RESULTS

A. The level scheme of ^{241}Pu

The thermal neutrons incident on a ^{240}Pu target undergo s-wave capture into a $\frac{1}{2}^+$ state in ^{241}Pu. In the γ-ray cascades that follow, levels with low spin are populated with greatest intensity. In the present work, the experimental sensitivity is expected to be sufficient to detect most levels from $I=\frac{1}{2}$ to $I=\frac{7}{2}$ and some of spin $\frac{9}{2}$ by combinations of secondary transitions. Primary transitions, which are predominantly of dipole character, populate medium and low-lying $I=\frac{1}{2}$ and $\frac{3}{2}$ levels. Since thermal capture in ^{240}Pu is dominated by a single resonance [23], the primary intensities are governed by Porter-Thomas fluctuations. Thus, some levels with appropriate spin and parity may not be populated with sufficient strength to appear in the primary spectrum.

The first step in interpreting the present data was the construction of a model-independent level scheme, based on the following principles: (a) the assumption that the existence of certain levels in the low-lying bands, those with energies between 0 and 301 keV, has been well established previously; (b) the use of the highly precise energies of secondary γ rays to derive level energies based on the Ritz combination principle; (c) the identification of levels populated by primary transitions from the capture state; (d) the independent confirmation of levels from α- and β-particle spectra, α- and β-decay γ rays, single-nucleon transfer reactions, inelastic deuteron scattering, and resonance neutron capture; (e) the use of the multipolarity data to specify or at least limit possible spin and parity assignments. Some application of the Alaga branching rules [24] has been made in confirming configuration assignments. These rules state that the ratio of reduced transition probabilities for γ-ray transitions of one multipolarity from a given state to any two members of a rotational band is independent of the intrinsic matrix elements and depends only on the ratio of two squared Clebsch-Gordan coefficients. This branching rule is valid only for states with relatively pure K quantum numbers and when $|K_i-K_f|\leq L\leq(K_i+K_f)$. Thus, we have not used this rule as a primary method for determining values of K or I, but it is cited in those instances where the observed branching ratios show good agreement with expected values.

Based on the present experimental data, 102 transitions (accounting for 64% of the observed transition intensity) were placed in a level scheme consisting of 54 levels. All levels assigned to ^{241}Pu are listed in Table V, along with a summary of the evidence for their existence. The level energies and uncertainties were determined by a least-squares fit of all assigned transition data [25] taken from the present (n,γ) studies. Also listed are the total observed transition strengths populating and depopulating each level. Model-independent spin/parity assignments are included. Configuration assignments are given for most levels, along with an assessment of the authors' confidence in that assignment. Depopulating transitions assigned to rotational bands are shown in Fig. 1.

In comparing with the previously measured secondary γ transitions in ^{241}Pu from thermal capture [14], we agree with 16 of the previous placements and we reject 6 placements because the γ rays do not appear in our spectra. The low-energy level structure of ^{239}U is very similar to that of ^{241}Pu. Of the 33 transitions placed by Börner *et al.* [1] in the level scheme of ^{239}U in order to define its level structure below 900 keV, we observe all of the corresponding γ transitions in ^{241}Pu, with 3 exceptions. In addition, we place another 36 transitions that depopulate these same levels.

With the inclusion of primary transitions in the level fit, we determined a neutron binding energy of 5241.57 ± 0.03 keV for ^{241}Pu. The major source of uncertainty is due to the systematic error in the Al γ rays used to calibrate the primary spectrum. This value is consistent with the value 5241.3 ± 0.7 keV derived from experimental systematics by Wapstra and Bos [26].

TABLE IV. Experimental differential cross sections for the ^{240}Pu$(d,p)^{241}$Pu and ^{242}Pu$(d,t)^{241}$Pu reactions.

	$d\sigma/d\Omega$ [a]				$d\sigma/d\Omega$ [b]		
E_{level} (keV)	(d,p) (μb/sr)	(d,t) (μb/sr)	Assigned config.	E_{level} (keV)	(d,p)	(d,t)	$(^3\text{He},\alpha)$
0	39(5)	47(5)	$\frac{5}{2}+\frac{5}{2}[622]$	0	w	m	
42(2)		6(2)	$\frac{7}{2}+\frac{5}{2}[622]$	43(2)		w	
96(1)	131(9)	214(10)	$\frac{9}{2}+\frac{5}{2}[622]$	94(1)	m	s	s
162(1)	38(5)	82(6)	$\frac{1}{2}+\frac{1}{2}[631]$	161(2)	w	m	
171(2)	78(7)	248(11)	$\frac{3}{2}+\frac{1}{2}[631]$	170(2)	m	vs	m
221(3)		11(3)	$\frac{5}{2}+\frac{1}{2}[631]$				
231(2)	38(5)	22(4)	$\frac{9}{2}+\frac{7}{2}[624]$	230(2)	w	w	
244(2)	13(3)	43(5)	$\frac{7}{2}+\frac{1}{2}[631]$	242(2)	w	w	m
301(2)		12(3)	$\frac{11}{2}+\frac{7}{2}[624]$	300(3)	w	vw	m
337(1)	34(5)	118(8)	$\frac{9}{2}+\frac{1}{2}[631]$	335(2)	w	m	s
373(2)		14(3)	$\frac{11}{2}+\frac{1}{2}[631]$	368(4)	vw	vw	
385(3)		6(2)	$\frac{13}{2}+\frac{7}{2}[624]$				
448(2)		20(3)	$\frac{11}{2}-\frac{7}{2}[743]$	445(4)	vw	w	w
505(2)			$\frac{13}{2}+\frac{1}{2}[631]$	499(3)			w
571(2)		47(5)	$\frac{15}{2}-\frac{7}{2}[743]$	571(3)	w	w	vs
755(1)	237(11)	18(3)	$\frac{1}{2}+\frac{1}{2}[620]$	752(3)	s	w	
770(1)		131(8)	$\frac{1}{2}-\frac{1}{2}[761]$	770(3)		m	
780(1)	148(9)	30(4)	$\frac{3}{2}-\frac{1}{2}[761]$	777(4)	s	w	
801(1)	228(11)	17(3)	$\frac{3}{2}+\frac{3}{2}[631]$	800(2)	vs	w	
801(1)	228(11)	17(3)	$\frac{5}{2}+\frac{1}{2}[620]$	800(2)	vs	w	
810(1)	130(9)	39(5)	$\frac{5}{2}-\frac{1}{2}[761]$	807(3)		m	
831(1)	201(11)	145(8)	$\frac{5}{2}+\frac{3}{2}[631]$	833(3)	s	m	s
831(1)	201(11)	145(8)	$\frac{7}{2}-\frac{1}{2}[761]$	833(3)	s	m	s
842(1)	176(10)	154(9)	$\frac{1}{2}^-[620]\otimes 0^-$	844(3)	m	s	
852(1)	93(12)	50(5)	$\frac{3}{2}^-[620]\otimes 0^-$				
863(2)	41(5)			864(3)	m	m	
877(2)	26(4)		$\frac{7}{2}+\frac{3}{2}[631]$	875(3)			m
898(2)	93(7)	25(4)	$\frac{9}{2}+\frac{1}{2}[620]$	897(4)	m	w	
918(2)	99(8)		$\frac{7}{2}^-[620]\otimes 0^-$	918(3)	m	w	
932(2)		76(6)					s
937(2)	97(8)		$\frac{9}{2}+\frac{3}{2}[631]$	936(3)	m	m	
950(3)	32(5)			948(5)	w	w	
965(1)		248(11)	$\frac{1}{2}-\frac{1}{2}[501]$	967(3)	m	s	
974(2)	100(8)			967(3)	m	s	
996(2)	56(6)	56(5)	$\frac{3}{2}-\frac{1}{2}[501]$	995(3)	w	w	m
996(2)	56(6)	56(5)	$\frac{11}{2}+\frac{3}{2}[631]$	995(3)	w	w	m
1008(2)		137(8)		1009(3)		m	
1020(3)	52(6)			1016(3)	m		
1062(3)		46(5)		1065(3)	w	w	
1084(3)	52(6)						
1090(3)		158(9)		1093(3)		m	m
1118(3)		32(4)		1121(3)		w	
1178(3)		109(7)		1179(3)		s	s
1206(3)	48(5)	126(8)		1206(4)	w	m	
1244(3)	$\sim$36			1242(4)	w		
1347(3)	41(5)			1344(4)	w		

TABLE IV. (*Continued*).

$d\sigma/d\Omega$ [a]				$d\sigma/d\Omega$ [b]			
E_{level} (keV)	(d,p) (μb/sr)	(d,t) (μb/sr)	Assigned config.	E_{level} (keV)	(d,p)	(d,t)	$(^3He,\alpha)$
1384(3)	78(7)			1381(4)	s		
1390(6)		62(6)		1396(3)		w	
1471(3)		30(4)		1474(3)		w	
1762(3)	147(10)			1759(3)	s	w	

[a]Present measurements: $E_d=12.0$ MeV (both measurements), $\theta(d,p)=90°$, $\theta(d,t)=150°$.
[b]Data taken from previous measurements [11,12]. Approximate cross-section magnitudes: very weak, weak, medium, strong, very strong. For $(^3He,\alpha)$, indication is of spectroscopic strength.

B. Assignment of Nilsson single-particle states to rotational bands

1. Level structure from model calculations and experimental comparisons

The arrangement of experimental levels into rotational bands and their assignment to Nilsson quantum states was guided in part by comparison with average-field theoretical calculations [27] and in part by comparison with studies of neighboring nuclei. In particular, the structure of ^{239}U [1] and ^{243}Cm [28], each of which differs from ^{241}Pu by a single proton pair, would be expected to show a comparable band structure. Of these, the experimental data currently available for ^{239}U provide a more detailed and more precise level scheme.

Many Nilsson model calculations of structures for deformed nuclei have been carried out using the traditional harmonic-oscillator form of the average nuclear potential. On the other hand, it has been found that use of a finite potential with a diffuse edge (Saxon-Woods) produces good agreement with experimental results, particularly in the actinide region, e.g., see Chasman *et al.* [29]. We have found the work published by Gareev *et al.* [27] provides the best correspondence with experimental results in the odd-mass actinides. They calculated excitation energies and configurations assuming a Saxon-Woods potential and including pairing correlations and quasiparticle-phonon interactions.

In the following subsections, we will first discuss assignment of the levels that constitute rotational bands in ^{241}Pu and assignment of each band to specific orbitals. These results are summarized in Table V and Fig. 2. Secondly, we will compare our experimental findings with theoretical calculations in the last subsection. These results are summarized in Table VI.

2. The ground state band $\frac{5}{2}^+[622]$:0, 42, 96, 161, and 235 keV

The ground state band of ^{241}Pu is assigned the configuration $\frac{5}{2}^+[622]$ based upon a measured spin, $J=\frac{5}{2}$ (paramagnetic resonance), and a measured magnetic moment [3]. Level energies measured in the present work generally agree with those from previous studies [1–11]. The lowest four levels in this band are defined by data from (n,γ)-, (d,p)-, (d,t)-, and $(^3He,\alpha)$-reaction studies, while the $I=\frac{13}{2}$ member at 235 ± 4 keV has been observed only in the $(^3He,\alpha)$ spectrum [9]. The ground state band in ^{239}U shows similar characteristics, i.e., level spacings and population in single-particle transfer reactions, and has also been assigned to the $\frac{5}{2}^+[622]$ orbital.

3. The $\frac{1}{2}^+[631]$ band: 162, 171, 223, 245, 335, 371, and 502 keV

The energies of the three lowest levels in this band, which have been measured in the present work, agree very well with those from previous studies [1–13]. We derive rotational parameters, $A=6.747$ keV and $a=-0.543$, from these energies. A new observation is the detection of a 221 ± 3-keV level in the (d,t) spectrum. Our thermal (n,γ) transition data define more precisely the energy of the $I=\frac{7}{2}$ band member, $E=244.889\pm0.001$ keV; this level was observed previously in transfer reaction data. No evidence has been found for a previously assigned, single γ-ray transition that defined the energy of this level as 242.7 keV [14]. Evidence for all of the higher spin members of this band comes from transfer-reaction studies. The previously assigned $I=\frac{9}{2}$ level at 335 ± 2 keV agrees with the present data. We find the $I=\frac{11}{2}$ member of the band, calculated to occur at 373.5 keV, to be best fit by a level at 371 ± 3keV that has been detected in the (d,t) spectrum and was previously assigned as $\frac{13}{2}^+\frac{7}{2}[624]$. The presently derived rotational parameters suggest the $I=\frac{13}{2}$ member of this $\frac{1}{2}^+[631]$ band should occur at 510 keV which raises some questions about the previous assignment of a level at 499 ± 3 keV observed in the $(^3He,\alpha)$ spectrum [9]. A new observation is a level at 505 ± 2 keV in the (d,t) spectrum. Perhaps both observations are of the $I=\frac{13}{2}$ level, one whose energy is still not well defined. A rotational band with similar characteristics occurs at 134 keV in ^{239}U and has also been assigned to the $\frac{1}{2}^+[631]$ orbital.

4. The $\frac{7}{2}^+[624]$ band: 175, 232, 301, and 385 keV

This configuration is populated in the favored α decay of ^{245}Cm. Studies of ^{245}Cm decay have defined the three lowest levels in the band [1–4]. Our thermal (n,γ) measurements provide precise energies for the two lowest levels. In these measurements, we did not detect the γ transitions seen in ^{245}Cm α decay to be depopulating the $I=\frac{11}{2}$ band member at 301 keV, probably because high-spin levels are populated so sparingly in cascades originating from an $I^\pi=\frac{1}{2}^+$ capture state. Taking into account the trend of a slightly decreasing rotational parameter with increasing spin, we calculate the $I=\frac{13}{2}$ band member to occur at 382 keV and assign a 385 ± 3-keV level, newly observed in the (d,t) spectrum, to this

TABLE V. Summary of evidence for excited levels in ^{241}Pu, including level energies, spin, parity, and Nilsson configuration assignments.

Adopted energy, spin [a]				Total trans. [b]		Other exptl. observations [c]							Nilsson
E_{lvl} (keV)	I_1^π	I_2^π	Ms.	In	Out	Prim. γ						Cf.	assign.
0.0	$\frac{5}{2}^+$	$\frac{5}{2}^+$		95.0				dp	dt		$\alpha\beta$	A	$\frac{5}{2}^+[622]$
41.972(1)	$\frac{7}{2}^+$	$\frac{7}{2}^+$	$n\gamma$	10.7	16.6				dt		α	A	$\frac{5}{2}^+[622]$
95.780(1)	$\frac{9}{2}^+$	$\frac{9}{2}^+$	$n\gamma$	2.8	4.3			dp	dt	$h\alpha$	α	A	$\frac{5}{2}^+[622]$
161.315(3)	$\frac{11}{2}^+$	$\frac{11}{2}^+$)	$n\gamma$	0.4	0.3			dp	dt	$h\alpha$	α	B	$\frac{5}{2}^+[622]$
235(4)	$\frac{13}{2}^+$		tr							$h\alpha$		B	$\frac{5}{2}^+[622]$
161.686(1)	$\frac{1}{2}^+$	$\frac{1}{2}^+$	$n\gamma$	27.4	60.5	161.72(2)	rc	dp	dt	$h\alpha$	α	A	$\frac{1}{2}^+[631]$
170.940(1)	$\frac{3}{2}^+$	$\frac{3}{2}^+$	$n\gamma$	20.0	2.7	169.7(10)		dp	dt	$h\alpha$		A	$\frac{1}{2}^+[631]$
222.988(1)	$\frac{5}{2}^+$	$\frac{5}{2}^+$	$n\gamma$	16.3	22.5				dt			A	$\frac{1}{2}^+[631]$
244.889(1)	$\frac{7}{2}^+$	$\frac{7}{2}^+$	$n\gamma$	1.2	5.7			dp	dt	$h\alpha$		A	$\frac{1}{2}^+[631]$
337.136(2)	$\frac{9}{2}^+$	$\frac{9}{2}^+$	$n\gamma$	0.5	1.0			dp	dt	$h\alpha$		B	$\frac{1}{2}^+[631]$
373(2)	$\frac{11}{2}^+$		tr					dp	dt			B	$\frac{1}{2}^+[631]$
505(2)	$\frac{13}{2}^+$		tr						dt	$h\alpha$		C	$\frac{1}{2}^+[631]$
175.052(1)	$\frac{7}{2}^+$	$\frac{7}{2}^+$	$n\gamma$	0.5	3.9						$\alpha\beta$	A	$\frac{7}{2}^+[624]$
231.934(8)	$\frac{9}{2}^+$	$(\frac{9}{2}^+)$	$n\gamma$		0.4			dp	dt		α	B	$\frac{7}{2}^+[624]$
301.176(16)	$\frac{11}{2}^+$		α					dp	dt	$h\alpha$	α	B	$\frac{7}{2}^+[624]$
385(3)	$\frac{13}{2}^+$		α						dt		α	C	$\frac{7}{2}^+[624]$
404.453(1)	$\frac{9}{2}^-$	$(\frac{7}{2},\frac{9}{2})^-$	$n\gamma$		1.8						β	A	$\frac{7}{2}^-[743]$
408.899(2)	$\frac{7}{2}^-$	$(\frac{7}{2},\frac{9}{2})^-$	$n\gamma$		0.3							B	$\frac{7}{2}^-[743]$
448(2)	$\frac{11}{2}^-$		tr					dp	dt	$h\alpha$		C	$\frac{7}{2}^-[743]$
571(2)	$\frac{15}{2}^-$		tr					dp	dt	$h\alpha$		C	$\frac{7}{2}^-[743]$
518.812(2)	$\frac{5}{2}^-$	$(\frac{5}{2},\frac{7}{2})^-$	$n\gamma$	0.4	4.1					dd'	β	A	$\frac{5}{2}[622]\otimes 0^-$
561.421(4)	$\frac{7}{2}^-$	$(\frac{7}{2},\frac{9}{2})^-$	$n\gamma$		1.2					dd'	β	A	$\frac{7}{2}[622]\otimes 0^-$
614.836(9)	$\frac{9}{2}^-$	$(\frac{5}{2},\frac{7}{2},\frac{9}{2})^-$	$n\gamma$		0.1					dd'		C	$\frac{9}{2}[622]\otimes 0^-$
755.174(2)	$\frac{1}{2}^+$	$\frac{1}{2}^+$	$n\gamma$	0.5	3.7	755.34(19)	rc	dp	dt			A	$\frac{1}{2}^+[620]$
784.152(2)	$\frac{3}{2}^+$	$\frac{3}{2}^+$	$n\gamma$	0.1	3.0	784.11(3)						A	$\frac{1}{2}^+[620]$
800.475(5)	$\frac{5}{2}^+$	$(\frac{3}{2},\frac{5}{2})^+$	$n\gamma$	0.5	2.9			dp	dt			A	$\frac{1}{2}^+[620]$
869.379(6)	$\frac{7}{2}^+$	$\frac{7}{2}^+$	$n\gamma$		1.0							C	$\frac{1}{2}^+[620]$
898(2)	$\frac{9}{2}^+$		tr					dp	dt			C	$\frac{1}{2}^+[620]$
769.268(3)	$\frac{1}{2}^-$	$(\frac{1}{2},\frac{3}{2})^-$	$n\gamma$	1.0	4.0	769.24(4)	rc		dt			A	$\frac{1}{2}^-[761]$
779.150(2)	$\frac{3}{2}^-$	$\frac{3}{2}^-$	$n\gamma$	1.1	5.4		rc	dp	dt			A	$\frac{1}{2}^-[761]$
810.945(3)	$\frac{5}{2}^-$	$\frac{5}{2}^-$	$n\gamma$		2.3			dp	dt			A	$\frac{1}{2}^-[761]$
833.353(4)	$\frac{7}{2}^-$	$(\frac{7}{2},\frac{9}{2},\frac{11}{2})^-$	$n\gamma$		0.5			dp	dt	$h\alpha$		B	$\frac{1}{2}^-[761]$
937(2)	$\frac{11}{2}^-$		tr					dp	dt			B	$\frac{1}{2}^-[761]$
800.452(5)	$\frac{3}{2}^+$	$\frac{3}{2}^+$	$n\gamma$	0.5	2.2	800.41(9)	rc	dp	dt			A	$\frac{3}{2}^+[631]$
831.588(7)	$\frac{5}{2}^+$	$(\frac{3}{2},\frac{5}{2})^+$	$n\gamma$		1.3			dp	dt	$h\alpha$		A	$\frac{3}{2}^+[631]$
877(2)	$\frac{7}{2}^+$		tr					dp		$h\alpha$		D	$\frac{3}{2}^+[631]$
937(2)	$\frac{9}{2}^+$		tr					dp	dt	$h\alpha$		C	$\frac{3}{2}^+[631]$
996(2)	$\frac{11}{2}^+$		tr					dp	dt	$h\alpha$		C	$\frac{3}{2}^+[631]$
841.957(2)	$\frac{1}{2}^-$	$(\frac{1}{2},\frac{3}{2})^-$	$n\gamma$	0.3	0.8	841.99(10)		dp	dt			A	$\frac{1}{2}[620]\otimes 0^-$
850.540(2)	$\frac{3}{2}^-$	$\frac{3}{2}^-$	$n\gamma$	0.3	2.1	850.56(3)	rc	dp	dt			A	$\frac{1}{2}[620]\otimes 0^-$
897.503(22)	$\frac{5}{2}^-$	$(\frac{1}{2},\frac{3}{2},\frac{5}{2})^-$	$n\gamma$		0.2			dp	dt			C	$\frac{1}{2}[620]\otimes 0^-$

TABLE V. (*Continued*).

Adopted energy, spin [a]				Total trans. [b]		Other exptl. observations [c]						Nilsson
E_{lvl} (keV)	I_1^π	I_2^π	Ms.	In	Out	Prim. γ					Cf.	assign.
918(2)	$\frac{7}{2}^-$		tr					dp	dt		C	$\frac{1}{2}[620]\otimes 0^-$
964.928(6)	$\frac{1}{2}^-$	$(\frac{1}{2},\frac{3}{2})^-$	$n\gamma$		1.9	964.92(1)	rc	dp	dt		A	$\frac{1}{2}^-[501]$
995.610(11)	$\frac{3}{2}^-$	$\frac{3}{2}^-$	$n\gamma$		1.3	995.69(4)	rc	dp	dt	$h\alpha$	B	$\frac{1}{2}^-[501]$
834.839(17)		$(\frac{3}{2},\frac{5}{2},\frac{7}{2})^+$	$n\gamma$		0.5					$h\alpha$	C	
940.309(9)		$(\frac{1}{2},\frac{3}{2})$	$n\gamma$		2.4	940.28(5)	rc				A	
942.584(5)		$(\frac{1}{2},\frac{3}{2})^+$	$n\gamma$		2.8	942.58(6)	rc				A	
1009.438(7)		$\frac{3}{2}^-$	$n\gamma$		0.9	1009.49(5)			dt		A	
1090.022(4)		$(\frac{1}{2},\frac{3}{2})^-$	$n\gamma$		0.5	1090.00(1)	rc		dt	$h\alpha$	A	
1223.839(9)		$(\frac{1}{2},\frac{3}{2})$	$n\gamma$		0.9	1223.74(6)		dp			B	
1253.790(6)		$(\frac{1}{2},\frac{3}{2})^-$	$n\gamma$		1.9	1253.80(1)		dp			A	
1268.855(23)		$(\frac{1}{2},\frac{3}{2})$	$n\gamma$			1268.86(2)		dp			B	
1296.671(6)		$\frac{3}{2}^-$	$n\gamma$		0.6	1296.73(1)		dp			B	
1357.663(15)		$(\frac{1}{2},\frac{3}{2})$	$n\gamma$		0.1	1357.65(1)					A	
5241.570(7)		$(\frac{1}{2},\frac{3}{2}^+)$	$n\gamma$								A	

[a]Adopted level energies are the best values derived from the experimental evidence summarized in this table. The energy listed in column 1 was measured using the technique shown in abbreviated form in the Ms. column (tr refers to single-nucleon transfer reaction spectroscopy). The levels appear in sequence according to their assignments in rotational bands. The column labeled I_1^π lists adopted spin and parity values derived from the Nilsson configurations listed in the last column of this table. The column labeled I_2^π lists model-independent spin-parity assignments made assuming that multipolarities of secondary transitions have either been measured or are limited to $E1$, $M1$, or $E2$ assignments. Parentheses enclose a range of possible I values; they do not indicate uncertainty.

[b]Column lists total transition strength populating and depopulating a given level in units of transitions per 100 neutron captures. The intensities of primary γ rays populating these levels are not included due to lack of an absolute calibration.

[c]Estimated confidence in the evidence for a level's configuration assignment is given in the column labeled Cf.: A denotes well established, B probable, C plausible.

band. This level has already been observed in the α-decay spectrum with an intensity that indicates a hindrance factor of $\geqslant 980$. This degree of hindrance is within an acceptable range for the $I=\frac{13}{2}$ member of a $K=\frac{7}{2}$ band being populated by favored α decay. There is reasonably good agreement between experiment and Alaga rules [24] for the branching ratios of the mostly dipole ($M1$) transitions between the $\frac{7}{2}^+$ bandhead and members of the $\frac{5}{2}^+[622]$ band. The rotational band assigned to the $\frac{7}{2}^+[624]$ orbital in ^{239}U is found at 169 keV.

5. The $\frac{7}{2}^-[743]$ band: 409($\frac{7}{2}$), 404($\frac{9}{2}$), 446($\frac{11}{2}$), and 570($\frac{15}{2}$) keV

Levels at 444 ± 3 and 569 ± 3 keV that were detected in single-particle transfer reactions [11,12] have been assigned previously to the $\frac{11}{2}$ and $\frac{15}{2}$ members, respectively, of this band. We detect negative-parity levels at 404.453 ± 0.001 and 408.899 ± 0.002 keV that we assign to the $I=\frac{9}{2}$ and $\frac{7}{2}$ members, respectively, of the band. The compressed nature of the rotational spacings observed here is understood to be the consequence of strong Coriolis mixing with levels in a $\frac{9}{2}^-[734]$ band that apparently lies just above the $K^\pi=\frac{7}{2}^-$ band. For the two close-lying levels at 404 and 409 keV, the question of spin assignments poses some problems. Both levels decay identically, each with three transitions that feed the same levels. For either level, the two transitions with higher energies feed the $I=\frac{7}{2}$ and $\frac{9}{2}$ levels of the ground-state band ($\frac{5}{2}^+[622]$). These transitions from the 404-keV level are quite intense, which suggests this level is a bandhead and may be accumulating transition strength from other members of the band or from related bands. Nevertheless, if we assign a $\frac{7}{2}^-\frac{7}{2}[743]$ configuration to this level, Alaga rules [24] suggest that the majority of the transition strength to the ground state band (75% of the reduced strength) should feed the $I=\frac{5}{2}$ bandhead, whereas this transition has not been detected in the GAMS spectrum. An attractive explanation for this observation is that the configuration of the 404-keV level is $\frac{9}{2}^-\frac{7}{2}[743]$, and that the Coriolis interaction has so depressed this level that it lies below the $I=\frac{7}{2}$ member of the band at 409 keV. In this case, the transition 404-keV level to ground, would be of $M2$ multipolarity which would *not* be expected to compete with the observed $E1$ transitions to higher-lying levels. At the same time, we are left with a comparable question about the 409-keV level, namely, where is the expected

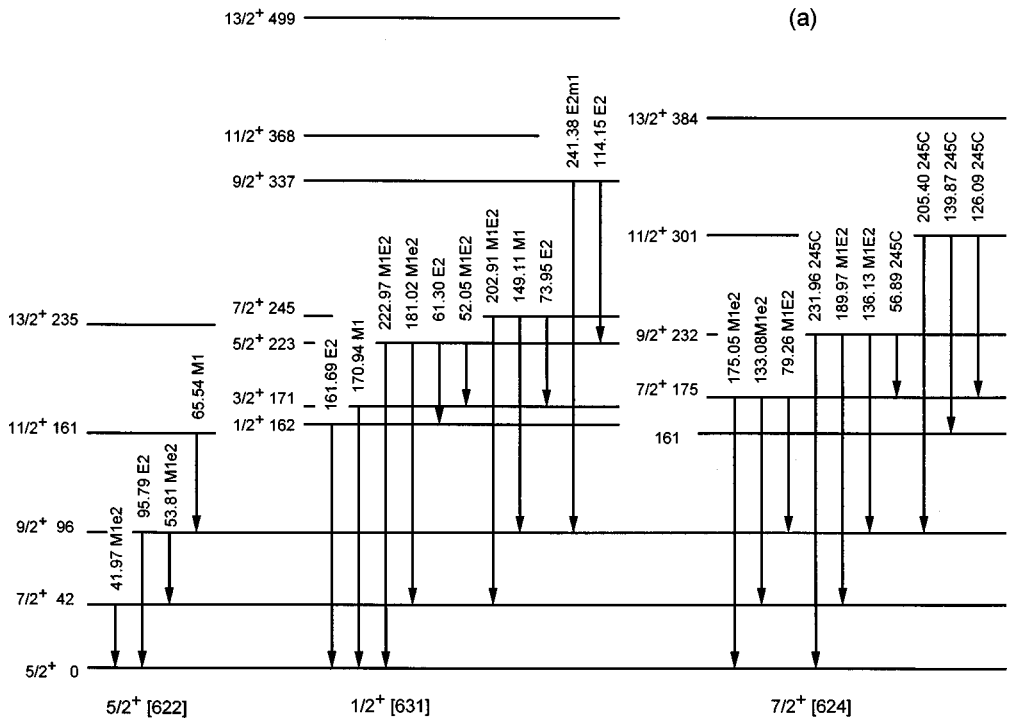

FIG. 1. Levels in ^{241}Pu assigned to rotational bands with Nilsson-configuration assignments and depopulating γ-ray transitions. Measured γ-ray energies (in keV) and multipolarities are shown. The notation of the multipolarities is explained in footnote e, Table I.

transition that feeds the ground state of ^{241}Pu? While its absence is as perplexing as for the 404-keV level, the transitions depopulating this higher level are much less intense and, hence, the ground-state transition may be more readily missed in our experiment. We know from the expected strength of the interaction between the $\frac{7}{2}[743]$ and $\frac{9}{2}[734]$ configurations that these two close-lying levels at 400 keV cannot both have $I^{\pi}=\frac{9}{2}$; if this were the case, we would expect an energy separation of 80–100 keV between them.

A Coriolis mixing calculation, summarized in Table VII, reproduces the present experimental level energies in the $\frac{7}{2}^{-}[743]$ band with good precision. This calculation was performed by first obtaining values for the parameters, $\hbar^2/2\mathfrak{I}=5.78$ keV and the interaction matrix element $A_{\frac{7}{2},\frac{9}{2}}=2.74$ keV, from a fitting of levels in ^{245}Cm in both the $\frac{7}{2}^{-}[743]$ and the $\frac{9}{2}^{-}[734]$ bands. These parameter values also produce a good fit to the three level energies assigned to the $\frac{7}{2}^{-}[743]$ orbital in ^{239}U, beginning at 293 keV.

Our initial mixing calculation of levels in ^{241}Pu was made assuming fixed values of the parameters, the same as found to produce good fits in ^{245}Cm and ^{239}U. This calculation (^{241}Pu I in Table VII) produced calculated energies for the $I=\frac{15}{2}$ levels in the two bands under discussion at 590 and 747 keV. For either level, one should expect to see strong peaks in the (d,p) spectrum since much of the single-particle strength of these configurations resides in the $I=\frac{15}{2}$ level. The lower of this pair has previously been assigned at 570 ± 2 keV from transfer reaction data. A satisfactory fit to all of the assigned levels in the $\frac{7}{2}^{-}[743]$ band (case II) was accomplished by allowing the rotational and mixing parameters to vary. In further calculations (cases III and IV), we show that reasonable fits may be made to the experimental data assuming the $\frac{15}{2}^{-}\frac{9}{2}[734]$ level occurs at either 800 or 777 keV. Although strong peaks in the (d,p) spectra appear at these energies, assignment of this level cannot be made with any certainty. The unobserved $\frac{9}{2}^{-}\frac{9}{2}[734]$ level is calculated to occur at 500 keV.

6. The $\frac{5}{2}^{-}[622]\otimes 0^{-}$ octupole vibration band: 519, 561, and 615 keV

The three states indicated have been previously observed in (d,d') reactions [11]. The lower two levels are known to be populated in ^{241}Np β^{-} decay [5–7]; they decay via $E1$ transitions to levels in the ground-state band. These data support the assignment of octupole vibrational character to this band [11]. The presence of low-lying octupole bands based on the $\frac{5}{2}^{+}[622]$ and $\frac{1}{2}^{+}[631]$ bands has been consistently demonstrated in the actinides [30]. In the present (n,γ) measurements, we might expect to find evidence for all three of these levels. While we are able to precisely define the energies of the lower two levels by their de-exciting $E1$ transitions, simple γ-ray combinations do not appear in the data for the level at 620 ± 10 keV. We derive a rotational parameter of 6.087 ± 0.001 keV from the observed $I=\frac{5}{2}$ to $\frac{7}{2}$ level spacing. This suggests the $I=\frac{9}{2}$ level should occur at $\sim$616.2 keV. We postulate this level decays to the 42-keV $\frac{7}{2}^{+}$ level by the emission of an $E1$ γ transition at 572.863 ± 0.009 keV. Transitions from this level, now placed at 614.8 keV, to the $\frac{9}{2}$ and $\frac{11}{2}$ levels in the ground-state band have not been observed. Of these, the transition to the $\frac{9}{2}$ level may be obscured by two somewhat more intense transitions at 518.810 and 519.433 keV. Based on this limited evidence, we tentatively assign an energy of 614.836 ± 0.009 keV to this level. γ-ray branching ratios for transitions between the two lowest levels in this band and members of the $\frac{5}{2}^{+}[622]$ ground-state band agree very well with expected values according to

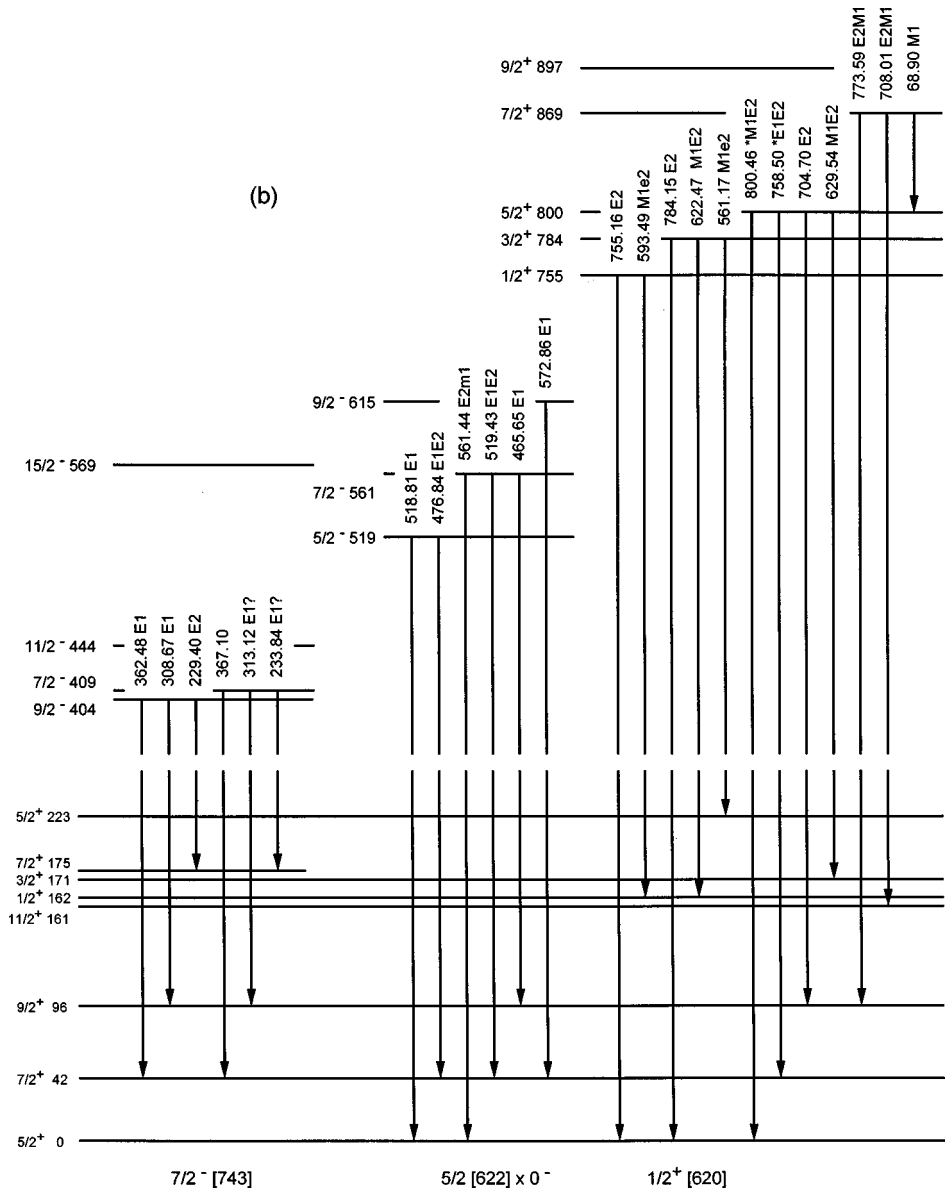

FIG. 1 (*Continued*).

Alaga rules [24]. An $I=\frac{5}{2}^{+}[622]$ level at 539 keV has been identified as the bandhead for this configuration in ^{239}U; energies of additional band members are not known.

7. The $\frac{1}{2}^{+}$[620] band: 755, 784, 800, 869, and 898 keV

The basic structure of this rotational band has been previously identified and assigned to a particle state, $\frac{1}{2}^{+}[620]$, on the basis of strong (d,p) population of these levels [11]. Our current assignment of levels agree with those made previously for the $I=\frac{1}{2},\frac{5}{2}$, and $\frac{9}{2}$ band members. We assign a new level at 784.152 ± 0.002 keV as the $I=\frac{3}{2}$ member of this band. Our (n,γ) data support a $\frac{1}{2}^{+}$ or $\frac{3}{2}^{+}$ assignment; also, we have a new identification of this level in the (d,p) spectrum. Present experimental data show the level at 769 keV, previously thought to belong in this band, to have negative parity with $I=\frac{1}{2}$ or $\frac{3}{2}$.

The $I=\frac{5}{2}$ band member at 800.475 ± 0.005 keV is apparently a member of a close-lying doublet that is just barely resolved in the interpretation of our (n,γ) data. The existence of this doublet was postulated in previous work [11,14]. Another new level from the present work that can be added to this band is the $I=\frac{7}{2}$ member at 869.379 ± 0.006 keV.

The five levels listed above define the $I=\frac{1}{2}$ to $\frac{9}{2}$ members of the $\frac{1}{2}^{+}[620]$ band. These experimental level energies are all precisely reproduced by rotational parameters $A=6.461$ keV and $a=+0.495$. The first four levels have been observed in our (n,γ) data and all five are populated by the (d,p) reaction. Three levels in ^{239}U have been assigned to this orbital; their spacings define a band with values for rotational parameters that are very similar to those of the presently discussed band in ^{241}Pu.

8. The $\frac{1}{2}^{-}[761]+\frac{1}{2}[631]\otimes0^{-}$ band: 769($\frac{1}{2}$), 779($\frac{3}{2}$), 811($\frac{5}{2}$), 833($\frac{7}{2}$), and 937($\frac{11}{2}$) keV

The bandhead listed above at 769 keV was previously observed in thermal and resonance neutron capture and was mistakenly thought to have positive parity. Our experimental

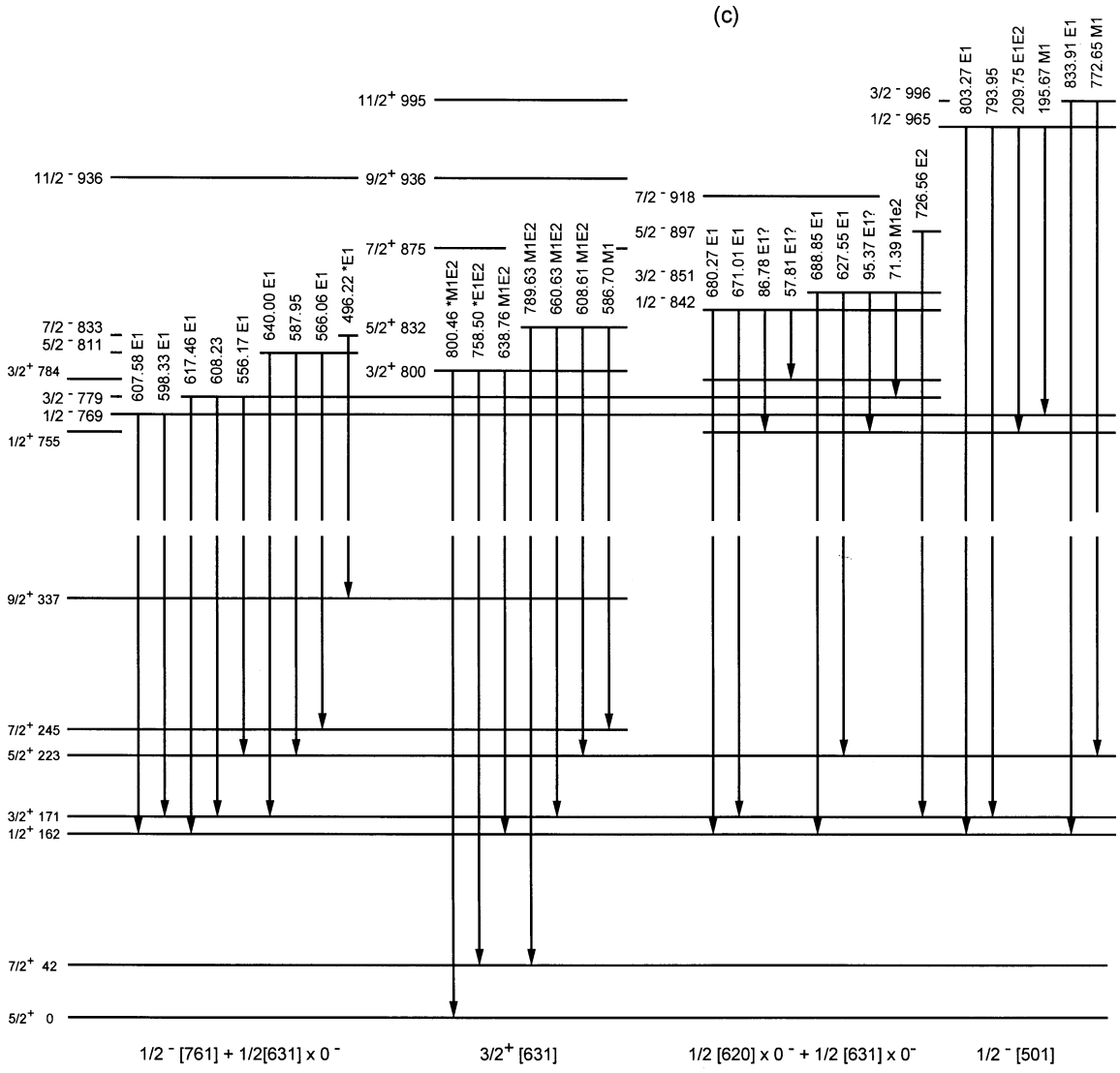

FIG. 1 (*Continued*).

(n,γ) data show spin and parity $I^{\pi}=\frac{1}{2}^{-}$ or $\frac{3}{2}^{-}$. The $I=\frac{3}{2}$ and $\frac{5}{2}$ members of this band, newly identified in our thermal (n,γ) data, decay to levels in the $\frac{1}{2}^{+}[631]$ band, as does the bandhead. With rotational parameters $A=4.827$ keV and $a=-0.318$, as derived from the energies of the three lowest levels, one calculates the $I=\frac{7}{2}$ level to occur at 834.0 keV. A level at 833 ± 2 keV, which is detected in all of the transfer reaction spectra, is assigned to the band. A single transition with energy 496.217$\pm$0.004 keV has been assigned to the de-excitation of this level to the $\frac{9}{2}^{+}\frac{1}{2}[631]$ level at 337 keV. Also, a level at 937$\pm$2 keV is assigned to the $I=\frac{11}{2}$ member of the band. As will be discussed in Sec. III B 12, this rotational band exhibits characteristics that are different from those expected from theoretical calculations. Its pattern of (d,p) intensities is most consistent with a $\frac{1}{2}^{-}[761]$ assignment. γ-ray branching ratios for transitions between the three lowest levels in this band and members of the $\frac{1}{2}^{+}[631]$ band agree rather precisely with expected values according to Alaga rules [24]. A comparable band occurring at 739 keV in ^{239}U has also been assigned to the $\frac{1}{2}^{-}[761]$ orbital.

9. The $\frac{3}{2}^{+}$[631] band: 800, 832, 877, 937, and 995 keV

In their study of ^{241}Pu levels with (d,t) and $(^{3}\mathrm{He},\alpha)$ reactions, Elze and Huizenga [12] assigned five levels beginning at 809 keV to a rotational band representing the $\frac{3}{2}^{+}[631]$ orbital. We should expect to find transitions in our thermal (n,γ) data that feed and depopulate at least the first two levels in this band, which are reported to occur at 809$\pm$3 and 835$\pm$3 keV. We do find evidence for an $I=\frac{3}{2}^{+}$ level at 800.452$\pm$0.005 keV and an $I=\frac{5}{2}^{+}$ level at 831.588$\pm$0.007 keV. The former is populated by a primary transition, which is indicative of $I=\frac{1}{2}$ or $\frac{3}{2}$. This $\frac{3}{2}^{+}$ level is the second member of a close-lying doublet discussed in Sec. III B 7. Our only level close in energy to 809 keV is an $I=\frac{5}{2}^{-}$ level at 810.945$\pm$0.003 keV, which has been assigned to the $\frac{1}{2}^{-}[761]$ rotational band. Thus, we reject the previous assignment of this bandhead at 809 keV, placing it now at 800 keV, and report a more precise energy for the $I=\frac{5}{2}$ member of the band [12]. The $I=\frac{7}{2}$ and higher levels in this $K^{\pi}=\frac{3}{2}^{+}$ band have been detected only in transfer reactions. As noted previously [12], the experimental differential cross

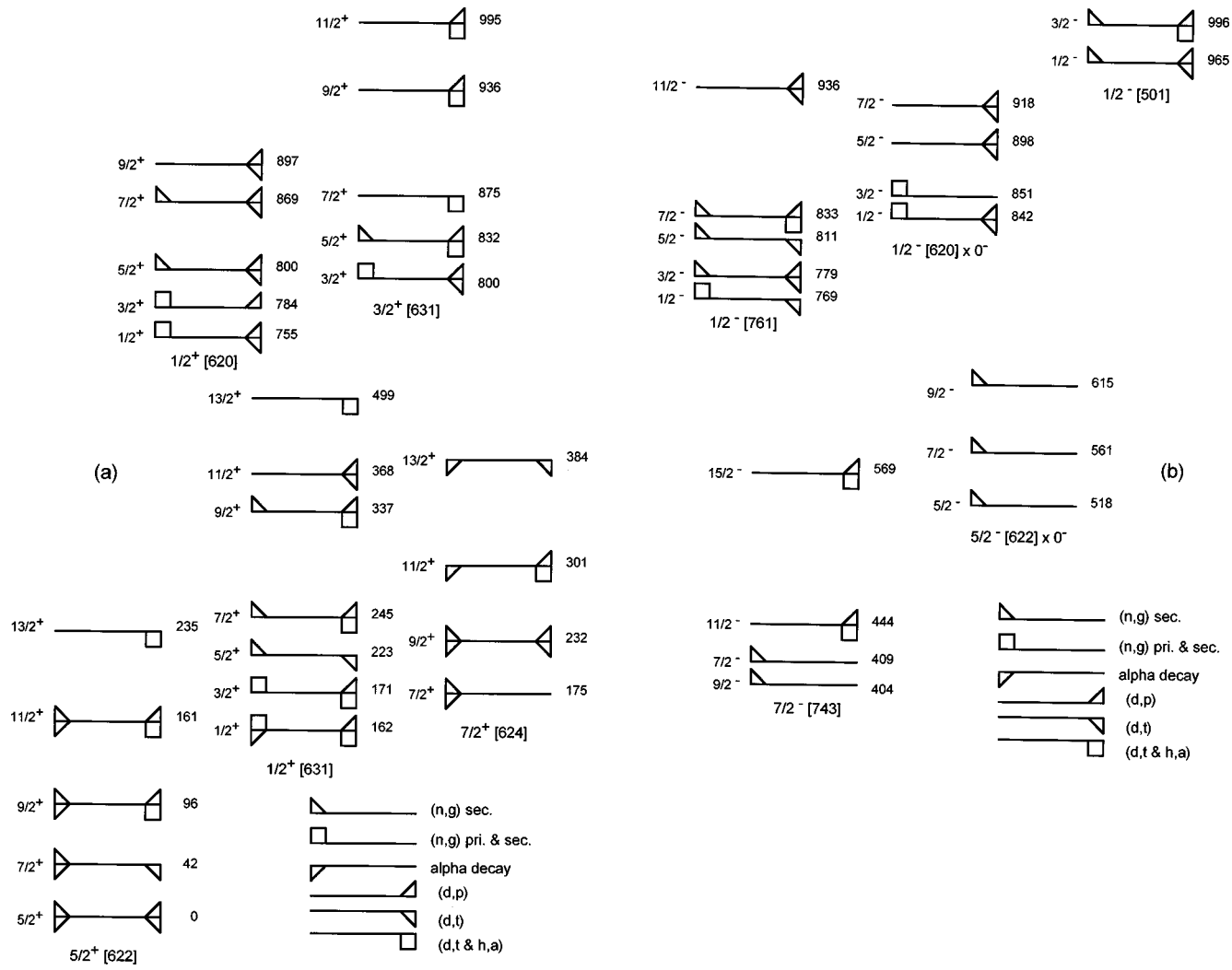

FIG. 2. Levels in ^{241}Pu assigned to rotational bands with Nilsson-configuration assignments and methods of experimental observation. For each level, assigned spin, parity, and level energy (in keV) are shown. (a) Positive-parity levels; (b) negative-parity levels.

sections for the (d,t) reaction fit reasonably well with calculated values for the $\frac{3}{2}^+[631]$ orbital.

This rotational band, as presently constituted, exhibits mostly consistent rotational spacing with $A=6.227(2)$ keV from the two lowest levels. Braid *et al.* [11] have shown that peaks occur in both the (d,p) and (d,t) spectra, corresponding to levels at 800 ± 2 and 807 ± 3 keV. They disagreed with the Elze-Huizenga assignments for this band, partly because the levels at 833 ± 3 and 955 ± 3 keV show comparable (d,p) and (d,t) cross sections. They have assigned just two levels to the $\frac{3}{2}^+[631]$ orbital, those at $(\frac{5}{2}^+)770\pm3$ keV and at $(\frac{9}{2}^+)864\pm3$ keV. In our data, we find evidence for an $I^\pi=\frac{1}{2}^-$ level at 769.268 ± 0.003 keV, but nothing to support the previously suggested $\frac{5}{2}^+$ level. In the (d,p) spectra, one finds very intense peaks at 801 ± 1 and 831 ± 1 keV, neither of which are apparently related to the presently considered orbital. Although one might assign the present band to the particle state $\frac{3}{2}^+[622]$, the fit to calculated cross sections (or spectroscopic factors) is poor.

10. The $\frac{1}{2}$[620]$\otimes0^-+\frac{1}{2}$[631]$\otimes0^-$ octupole vibration band: 842, 851, 898, and 918 keV

The two lowest levels assigned to this band were detected in previous studies of thermal and resonance *primary* γ rays, but their parity was either undetermined or mischaracterized as positive. In our (n,γ) measurements, we detect both primary and secondary γ rays feeding and de-exciting levels at 841.957 ± 0.002 and 850.540 ± 0.002 keV. The measured conversion coefficients of these secondary γ rays indicate a series of $E1$ transitions, supporting evidence for negative parity assignments to these levels. Secondary γ rays that de-excite the $I=\frac{5}{2}$ member of this band at 897.503 ± 0.022 keV were also detected. From these level energies, we obtain rotational parameters $A=6.127$ keV and $a=-0.533$. From these parameters, we calculate the $I=\frac{7}{2}$ band member to occur at 917.5 keV. This energy agrees well with a level at 918 ± 2 keV that is found in the (d,p) spectra, indicating some nonvibrational component in this band. A discussion of the configuration of this band, which apparently includes the vibrational components shown above, is given in Sec. III B 12.

11. The $\frac{1}{2}^-$[501] band: 965 and 966 keV

The first two levels of a $K^\pi=\frac{1}{2}^-$ band have been detected beginning at 965 keV. Most of the transition strength depopulating these levels leads to members of the $\frac{1}{2}^+[631]$ band. These levels are also populated by thermal (n,γ) pri-

TABLE VI. Characteristics of rotational bands in ^{241}Pu and ^{239}U.

Experimental			Theoretical [a]			Experimental	
	Bandhead energy (keV)			% Indic.	Other		Rotational parameters (keV)
Config.	241Pu	239U	Theory	config.	components	Nuclide	A_{expt} [b]
$\frac{5}{2}^+[622]$	0.0	0.0	0	90%	minor	^{241}Pu	5.996(1),5.979(1),5.941(1)
						^{239}U	6.078(1), **6.232(3)**
						^{235}U	6.013(1),6.003(1),5.975(2)
$\frac{1}{2}^+[631]$	161.7	133.8	50	88%	minor	^{241}Pu	6.747(1), $a=-0.543(1)$
						^{239}U	6.817(1), $a=-0.414(1)$
$\frac{7}{2}^+[624]$	175.1	169.1	60	82%	minor	^{241}Pu	6.312(1), 6.279(7)
						^{239}U	6.36(17), **6.86(21)**
$\frac{7}{2}^-[743]$	408.9	292.6	170	91%	minor	^{241}Pu	–, 3.78(27), –, 4.43(13)
						^{239}U	–, 4.01(13), –, 4.50(9)
$\frac{5}{2}[622]\otimes 0^-$	518.8	539.3	590	16%	60% $\frac{5}{2}[752]$	^{241}Pu	6.087(1), 5.935(11)
						^{239}U	
$\frac{1}{2}^+[620]$	755.2	687.9	710	50%	38% $[622]\otimes 2^+$	^{241}Pu	6.461(1), $a=+0.495(1)$
						^{239}U	6.546(5), $a=+0.425(5)$
$\frac{1}{2}^-[761]$	769.3	739.4	670		43% $\frac{1}{2}[501]$	^{241}Pu	4.827(1), $a=-0.318(1)$
$+\frac{1}{2}[631]\otimes 0^-$					29% $[631]\otimes 0^-$	^{239}U	4.934(3), $a=-0.550(1)$
$\frac{3}{2}^+[631]$	800.4	726.1	620		50% $\frac{3}{2}[622]$	^{241}Pu	6.227(2)
					36% $[624]\otimes 2^+$	^{239}U	6.209(6)
$\frac{1}{2}[620]\otimes 0^-$	842.0	815.2	900	37%	24% $\frac{1}{2}[501]$	^{241}Pu	6.127(3), $a=-0.533(1)$
$+\frac{1}{2}[631]\otimes 0^-$					29% $[631]\otimes 0^-$	^{239}U	
$\frac{3}{2}^+[622]$		853.2	1060		69% $[631]\otimes 2^+$	^{239}U	6.97(6)
					19% $\frac{3}{2}[631]$		
$\frac{1}{2}^-[501]$	964.9	932.9	1200		33% $[631]\otimes 0^-$	^{241}Pu	$\sim$6.5, $a\approx+0.57$
					32% $\frac{1}{2}[770]$	^{239}U	6.93(11), $a=+0.392(20)$
$\frac{3}{2}[631]\otimes 2^+$		965.6					
$\frac{1}{2}[631]\otimes 0^+$		1155.1					
$\frac{1}{2}[750]$		1194.6					

[a]Bandhead energies, configurations taken from Ref. [27].

[b]For A_{expt}, uncertainties in the last digits are in parentheses. The rotational parameters are calculated with the formula $A_{expt}=[E(2)-E(1)]/\{I(2)[I(2)+1]-I(1)[I(1)+1]\}$. Experimental rotational parameters , when known, are given for each band in ^{241}Pu and also for the same configuration in the isotonic nucleus ^{239}U and, in one instance, ^{235}U. Parameters in bold type are those that violate the regular trend of slightly decreasing A with increasing angular momentum exhibited in an isotone.

mary transitions and in both the (d,p) and (d,t) reactions. If we assume a rotational parameter A$\approx$6.5 keV for this band, the decoupling constant is approximately $+0.6$ while the calculated value for a $\frac{1}{2}^+[501]$ band is $+1.0$. [27].

12. Experimental versus theoretical level structure comparison

As already mentioned, we have found the calculations of Gareev *et al.* [27] to provide the best comparison of theoretical level structure with experiment. Another theoretical treatment that provides explicit energies for comparison with experiment is that of Libert *et al.* [31] whose self-consistent calculations were performed within the Hartree-Fock plus BCS approximation using the Skyrme SIII phenomenological effective force. While the Libert *et al.* calculations provide rather good agreement between calculated energies and experiment for the four lowest energy configurations in ^{241}Pu, the higher lying structure is not predicted accurately, possibly because vibrational excitations have not been included in the model. Nevertheless, even the limited success of the Libert *et al.* model is impressive in view of the fact that they employed a very small set of phenomenological parameters. For our purposes, we will use the more realistic model of Gareev *et al.* in order to make detailed comparisons between experiment and theory. These are summarized in Table VI. In the following discussion, all references to calculated or theoretical structure in ^{241}Pu are to the work of Gareev *et al.* [27].

There is good agreement between calculated excitation energies and experiment for the first four configurations found in ^{241}Pu, namely, the $\frac{5}{2}^+[622]$, $\frac{1}{2}^+[631]$, $\frac{7}{2}^+[624]$, and $\frac{7}{2}^-[743]$ bands. These configurations are calculated to have the least amount of configuration mixing. It is clear from the observed level spacings in the $\frac{7}{2}^-[743]$ band that the levels are interacting strongly with those in another band(s), in this case, the $\frac{9}{2}^-[734]$ band. Theoretical calculations suggest a spacing of 190 keV between bandheads; our Coriolis calculations, in which all of the observed $\frac{7}{2}^-[743]$ levels are precisely fit, place the $\frac{9}{2}^-$ band at 100 keV above the $\frac{7}{2}^-$ band. The $\frac{1}{2}^+[620]$ band, found experimentally at 755 keV, seems to display the characteristics predicted theo-

TABLE VII. Level-energy fitting calculations for two $j=\frac{15}{2}$ bands in ^{241}Pu, ^{245}Cm, and ^{239}U, including Coriolis mixing effects.

	Calc: ^{241}Pu I				Calc: ^{241}Pu II				Calc: ^{241}Pu III			
	$\frac{7}{2}[743]$		$\frac{9}{2}[734]$		$\frac{7}{2}[743]$		$\frac{9}{2}[734]$		$\frac{7}{2}[743]$		$\frac{9}{2}[734]$	
	$E_{\text{exp.}}$	$E_{\text{calc.}}$	$E_{\text{exp.}}$	$E_{\text{calc.}}$	$E_{\text{exp.}}$	$E_{\text{calc.}}$	$E_{\text{exp.}}$	$E_{\text{calc.}}$	$E_{\text{exp.}}$	$E_{\text{calc.}}$	$E_{\text{exp.}}$	$E_{\text{calc.}}$
	Fitted level energies (keV)											
$E\frac{7}{2}$	408.9	408.9			408.9	408.9			408.9	408.9		
$E\frac{9}{2}$	404.5	404.5		480.2	404.5	404.5		499.7	404.5	404.0		504.7
$E\frac{11}{2}$		453.7		558.6		445.7		586.1	444	444.8		593.9
$E\frac{13}{2}$		515.9		647.2		501.4		681.2		500.7		691.8
$E\frac{15}{2}$		590.3		746.8	570	570.0		786.6	570	569.8	800	800.0
	Fitted parameters (keV) [a]											
$E\frac{9}{2}[734]$		423.6				443.1				446.5		
$\hbar^2/2\mathfrak{I}$										5.91		
$A\frac{7}{2},\frac{9}{2}$						3.89	(6.76)			4.15	(6.76)	
	Fixed parameters (keV) [a]											
$E\frac{7}{2}[743]$		408.9				408.9				408.9		
$\hbar^2/2\mathfrak{I}$		5.80				5.80						
$A\frac{7}{2},\frac{9}{2}$		2.74	(6.76)									

	Calc: ^{241}Pu IV				Calc: ^{245}Cm				Calc: ^{239}U			
	$\frac{7}{2}[743]$		$\frac{9}{2}[734]$		$\frac{7}{2}[743]$		$\frac{9}{2}[734]$		$\frac{7}{2}[743]$		$\frac{9}{2}[734]$	
	$E_{\text{exp.}}$	$E_{\text{calc.}}$	$E_{\text{exp.}}$	$E_{\text{calc.}}$	$E_{\text{exp.}}$	$E_{\text{calc.}}$	$E_{\text{exp.}}$	$E_{\text{calc.}}$	$E_{\text{exp.}}$	$E_{\text{calc.}}$	$E_{\text{exp.}}$	$E_{\text{calc.}}$
	Fitted level energies (keV)											
$E\frac{7}{2}$	408.9	408.9			643.5	643.5			292.6	292.6		
$E\frac{9}{2}$	404.5	405.6		496.2	701.7	702.9	388.1	388.4		325.4		463.4
$E\frac{11}{2}$	444	447.2		580.6	775.0	775.1	442.8	443.4	372.7	371.1		545.3
$E\frac{13}{2}$		503.0		673.6		859.8	508.7	509.0		429.2		638.0
$E\frac{15}{2}$	570	571.5	777	776.9		957.0		585.3	498.6	499.2		742.0
$E\frac{17}{2}$						1066.4		672.4		581.0		857.4
	Fitted parameters (keV) [a]											
$E\frac{9}{2}[734]$		441.4				395.8				444.0		
$\hbar^2/2\mathfrak{I}$		5.73				5.78						
$A\frac{7}{2},\frac{9}{2}$		3.69	(6.76)			2.74	(6.74)					
	Fixed parameters (keV) [a]											
$E\frac{7}{2}[743]$		408.9				643.5				292.6		
$\hbar^2/2\mathfrak{I}$										5.80		
$A\frac{7}{2},\frac{9}{2}$										2.76	(6.78)	

[a]Theoretical values for the GM matrix elements, taken from Ref. [29], are shown in parentheses.

retically, namely, a configuration consisting of 50% $\frac{1}{2}^+[620]$, 38% $[622]\otimes 2^+$, plus other, minor components. The observed patterns of (d,p) population among band members and of γ rays deexciting band members are in qualitative agreement with the calculated microscopic structure of this band.

We will discuss next some significant deviations from predicted structures in rotational bands that occur mostly at higher excitations. The experimental evidence for the $K^\pi=\frac{5}{2}^-$ band at 519 keV is consistent with a purely vibrational band, e.g., no population of levels by transfer reactions is detected. Presumably, the configuration of this band is $\frac{5}{2}[622]\otimes 0^-$. Gareev *et al.* calculate the lowest $\frac{5}{2}^-$ band in ^{241}Pu to have only 16% of this vibrational character with the predominant configuration being 60% $\frac{5}{2}^-[752]$. If this latter configuration were important in this band, we might expect to detect transitions feeding levels in the $\frac{7}{2}^-[743]$ band. These have not been detected. Also, we might expect to see considerable (d,t) and $(^3\text{He},\alpha)$ strength in the $I=\frac{15}{2}$ member of a $\frac{5}{2}^-[752]$ band, in this instance, expected at approximately 849 keV. We have not been able to identify this. There does exist a fairly strong peak in the (d,t) spectrum at 842 ± 1keV, but no corresponding peak in the $(^3\text{He},\alpha)$ spectrum. It appears that the calculations have underestimated the purity of this $\frac{5}{2}[622]\otimes 0^-$ band.

There are five $K^\pi=\frac{1}{2}^-$ orbitals that are likely to appear below 1 MeV excitation in ^{241}Pu, namely, $\frac{1}{2}^-[761]$, $\frac{1}{2}^-[750]$, $\frac{1}{2}^-[501]$, $\frac{1}{2}[631]\otimes 0^-$, and $\frac{1}{2}[620]\otimes 0^-$. We have observed three $K^\pi=\frac{1}{2}^-$ bands in ^{241}Pu below 1 MeV. Our present data suggest that configuration mixing plays an im-

portant role in the $K^\pi = \frac{1}{2}^-$ bands that we have identified and that these configurations do not necessarily arise in the sequence calculated theoretically.

The lowest $K^\pi = \frac{1}{2}^-$ band in ^{241}Pu is calculated to occur at 670 keV and to consist predominantly of two configurations, 43% $\frac{1}{2}^-[501]$ and 29% $\frac{1}{2}[631]\otimes 0^-$. Experimentally, we observe the lowest $\frac{1}{2}^-$ band at 769 keV. All of the deexciting transitions of band members feed levels in the $\frac{1}{2}^+[631]$ band, consistent with what is expected for a vibrational state built upon this single-particle state. At the same time, the observed pattern of (d,p) population of the band, rather strong peaks for the $I = \frac{3}{2}$, $\frac{7}{2}$, and $\frac{11}{2}$ levels alternating with weaker upper limits for the other levels, agrees well with that expected for the $\frac{1}{2}^-[761]$ orbital. Certain levels in the band are also apparently strongly populated by (d,t) reactions, behavior that is inconsistent with a rather high-lying particle state ($\frac{1}{2}^-[761]$). The observed decoupling parameter, -0.318, does not agree with a theoretical value of -4.5 for the $\frac{1}{2}^-[761]$ orbital nor with a theoretical value of $+1.0$ for the $\frac{1}{2}^-[501]$ orbital, although mixing between these orbitals may explain the experimental value. Apparently this rotational band cannot be categorized simply as representing a single neutron orbital. Our observations appear to be consistent with the presence of several configurations in the mix that represents this band.

The next $K^\pi = \frac{1}{2}^-$ band in ^{241}Pu occurs at 842 keV, close to the calculated value of 900 keV. Its principal components are calculated to be the same as those of the previous band, 24% $\frac{1}{2}^-[501]$ and 37% $\frac{1}{2}^+[631]\otimes 0^-$. From the observed level energies, we obtain rotational parameters $A = 6.127$ keV and $a = -0.533$. These values, not so different from those of the $\frac{1}{2}^+[631]$ band (at 162 keV), and the existence of $E1$ transitions (with energies in the range 600–700 keV) that populate the $\frac{1}{2}^+[631]$ band suggest a $\frac{1}{2}[631]\otimes 0^-$ configuration assignment. On the other hand, much lower energy transitions, i.e., with energies <100 keV, are seen to be feeding levels in the $\frac{1}{2}^+[620]$ band. Since these transitions are able to compete with others of much higher energy and, thus, are several hundred times more probable after correction for energy dependence, it suggests the configuration of the present band includes a significant amount of a $\frac{1}{2}[620]\otimes 0^-$ vibrational state. This observation goes against theoretical predictions where the $\frac{1}{2}[620]\otimes 0^-$ configuration does not play an important role in any of the levels calculated below 1200 keV [27]. It is interesting to note that the two low-energy transitions between the 842.0-keV bandhead and levels in the $\frac{1}{2}^+[620]$ band exhibit a ratio close to the theoretical value given by the Alaga rules [24], while transitions from this level and the 850.5-keV band member to levels in the $\frac{1}{2}^+[631]$ band *do not* match expected values. Also, the levels in this band appear to receive some (d,p) and (d,t) population, including the $I = \frac{7}{2}$ member at 918 keV. Some of this behavior may be explained by the existence of more than one level at a given energy, e.g., the $\frac{9}{2}^+\frac{1}{2}[620]$ level at 898 ± 3 keV seen in transfer reactions and the $\frac{5}{2}^-$ level in the present band at 897.503 keV seen in the thermal (n,γ) data. The relative (d,t) cross sections can be fit at least partially by those calculated for a $\frac{1}{2}^-[501]$ orbital. On the other hand, one can rule out a $\frac{1}{2}^-[761]$ component since there is no match with what is expected for this configuration. Detailed theoretical calculations could help to determine how to apportion the observed transfer reaction strength between two different levels. Thus, the rotational band being considered here is thought to exhibit a mixed configuration with two of the important components being vibrational, namely, $\frac{1}{2}[631]\otimes 0^-$ and $\frac{1}{2}[620]\otimes 0^-$, and with some nonvibrational component(s) in order to account for the (d,p) and (d,t) population.

The third $K = \frac{1}{2}^-$ band, calculated to occur at 1200 keV and defined experimentally by only two levels beginning at 965 keV, is assigned to the $\frac{1}{2}^-[501]$ orbital, which is consistent with the deduced value of its decoupling constant. This assignment does not imply that other modes are not mixed into this band's configuration; the sparse data make further assignment questionable. The levels decay predominantly to members of the $\frac{1}{2}^+[631]$ band, as do the levels in the two previously discussed bands. A strong (d,t) peak for the $I = \frac{1}{2}$ level is observed and is again consistent with a $\frac{1}{2}^-[501]$ assignment, whereas the observed moderate (d,p) strength must arise from some other configuration in this mixture. Gareev *et al.* calculate about 33% contributions of $\frac{1}{2}^-[770]$ and $\frac{1}{2}[631]\otimes 0^-$ orbitals for this band. While the occurrence of the former orbital is not obvious from our data, limited as they are, the observed gamma decay of these levels is consistent with the proposed vibrational component.

IV. CONCLUSIONS

Our study of ^{241}Pu, along with the data of previous investigators, has allowed the assignment of configurations to 10 rotational bands, which are comprised of 44 levels. Evidence for the existence of these levels has come mainly from γ-spectroscopic measurements of primary and secondary transitions in thermal neutron capture and from (d,p) and (d,t) reaction spectroscopy. There is also evidence for 11 additional levels that have not been given configuration assignments. A total of 102 transitions out of measured 237 secondary lines (or 64% of the total transition strength) were placed in the decay scheme.

As can be seen in Table VI, there is excellent correspondence between the excitation energies and values of rotational parameters of the experimentally determined bands in ^{241}Pu and ^{239}U, especially for bands lying below 1 MeV. The average difference in band energies between these two nuclei is 45 keV; the average difference in rotational parameters for the six cases where data exist and where perturbations due to Coriolis interactions are minimal is 1.2%. In all but one case, the rotational parameter of the band in ^{241}Pu is smaller (or the moment of inertia is larger) due to the added proton pair. In their study of ^{238}U$(n,\gamma)^{239}$U, Börner *et al.* [1] detected five transitions in the energy range 1000–1070 keV whose conversion coefficients indicated a significant $E0$ component, along with $M1$ and $E2$ character. These transitions were combined with others to define four levels that were assigned to β-vibrational bands built upon the ground-state $\frac{5}{2}^+[622]$ band and upon the $\frac{1}{2}^+[631]$ band. In our measurements, we have identified only three transitions whose conversion coefficients suggest an $E0$ component; these occur at rather disparate energies. None have been placed in the decay scheme.

The energies and structures of excited states in ^{241}Pu calculated by Gareev *et al.* [27] correspond to experiment reasonably well for most states below 1 MeV excitation. Those states that are largely single-particle in character are well reproduced by the model. Nevertheless, three such states, predicted to occur at relatively low excitation energies, have not been identified in the present study. The lowest of these, a $\frac{9}{2}^-[734]$ orbital calculated to occur at 360 keV, has been placed at approximately 500 keV in the Coriolis mixing calculations summarized in Table VII. The most likely form of de-excitation for this bandhead will be $M1$ transitions to the $\frac{7}{2}^-[743]$ levels at 404 and 409 keV; these transitions have not been identified in our neutron capture spectrum. Two additional unidentified states, both arising from the same spherical state, with Nilsson quantum numbers $\frac{5}{2}^+[633]$ and $\frac{9}{2}^+[615]$ are predicted to occur at 530 and 640 keV, respectively. Each of these bandheads would be expected to exhibit transitions to the $I=\frac{7}{2}$ and $\frac{9}{2}$ levels of the $\frac{7}{2}^+[624]$ orbital, but none have been identified.

Some deviations from calculation begin to appear in states observed at higher excitations as configuration mixing becomes prevalent. For example, calculations predict the lowest $K^\pi=\frac{5}{2}^-$ band will occur at 590 keV and will have 60% $\frac{5}{2}^-[752]$ character, with just 16% $\frac{5}{2}[622]\otimes 0^-$ vibrational character. Experimentally, we observe a state at 519 keV that has apparently rather pure $\frac{5}{2}[622]\otimes 0^-$ character with little or no evidence of $\frac{5}{2}^-[752]$ mixing, i.e., we observe neither a pattern of de-excitations to levels in the $\frac{7}{2}^-[743]$ band nor strength in both the (d,t) and (h,α) reactions that would indicate $\frac{5}{2}^-[752]$ character.

In an analogous manner, there are significant differences between the experimentally observed characteristics of the three lowest energy $K^\pi=\frac{1}{2}^-$ rotational bands and those calculated by Gareev *et al.* In this case, the observables that could be compared with theory included the decoupling parameter of the band, de-excitation paths, and transfer-reaction cross sections. It was found that while there was a general correspondence between experimental behavior and theory for these bands, detailed predictions of mixing were often not borne out. A more complete discussion of this phenomenon is given in Sec. III B 12.

ACKNOWLEDGMENTS

One of the authors (D.H.W.) wishes to express his thanks to the Institut Laue-Langevin and Western Oregon University for financial support during his stay in Grenoble. Work performed in part under the auspices of the U.S. Department of Energy by the Lawrence Livermore National Laboratory under Contract No. W-7405-ENG-48 and by the Argonne National Laboratory under Contract No. W-31-109-ENG-38. The authors thank R.W. Lougheed and R.J. Dougan for isolating pure samples of ^{245}Cm from ^{249}Cf α decay. We thank Dr. Y. Akovali for helpful discussions regarding ^{245}Cm α decay. The authors are indebted for the use of isotopically pure ^{240}Pu target material to the Division of Chemical Sciences, Office of Basic Energy Sciences, U.S. Department of Energy, through the Calutron facilities of the Oak Ridge National Laboratory.

[1] H. G. Börner, H. R. Koch, H. Seyfarth, T. von Egidy, W. Mampe, J. A. Pinston, K. Schreckenbach, and D. Heck, Z. Phys. A **286**, 31 (1978).
[2] M. R. Schmorak, Nucl. Data Sheets **66**, 839 (1992); **40**, 1 (1983).
[3] Y. A. Ellis-Akovali, Nucl. Data Sheets **44**, 407 (1985); Y. A. Akovali, *ibid.* **72**, 191 (1994).
[4] S. A. Baranov and V. M. Shatinskii, Sov. J. Nucl. Phys. **22**, 346 (1976).
[5] A. M. Friedman and J. Milsted, Phys. Lett. **21**, 179 (1966).
[6] J. K. Dickens and J. W. McConnell, Phys. Rev. C **22**, 1344 (1981).
[7] S. A. Baranov, Y. F. Rodionov, V. M. Kulakov, and V. M. Shatinskii, Yad. Fiz. **4**, 1108 (1966); Sov. J. Nucl. Phys. **4**, 798 (1967).
[8] P. P. Parekh, E.-M. Franz, S. Katcoff, and L. K. Peker, Phys. Rev. C **24**, 2240 (1981); **25**, 2137(E) (1982).
[9] S. A. Qaim, Nucl. Phys. **88**, 285 (1966).
[10] R. Vandenbosch, Phys. Rev. **113**, 259 (1959).
[11] T. H. Braid, R. R. Chasman, J. R. Erskine, and A. M. Chasman, Phys. Rev. C **6**, 1374 (1972).
[12] Th. W. Elze and J. R. Huizenga, Phys. Rev. C **3**, 234 (1971).
[13] S. W. Yates, I. Ahmad, A. M. Friedman, F. J. Lynch, and R. E. Holland, Phys. Rev. C **11**, 599 (1975).
[14] P. Matussek, *Proceedings of the 2nd International Symposium on Neutron Capture Gamma Ray Spectroscopy and Related Topics*, Petten, The Netherlands, 1974, edited by K. Abrahams, F. Stecher-Rasmussen, and P. Van Assche (Reactor Centrum, Nederland, 1975), p. 655.
[15] C. Weitkamp, P. Matussek, and H. Ottmar [14], p. 749.
[16] B. W. Thomas and T. J. Haste [14], p. 670.
[17] H. R. Koch, H. G. Börner, J. A. Pinston, W. F. Davidson, J. Faudou, R. Roussille, and O. W. B. Schult, Nucl. Instrum. Methods **175**, 401 (1980).
[18] W. Mampe, K. Schreckenbach, P. Jeuch, B. P. K. Maier, F. Braumandl, J. Larysz, and T. von Egidy, Nucl. Instrum. Methods **154**, 127 (1978).
[19] R. S. Hager and F. C. Selzer, Nucl. Data, Sect. A **4**, 1 (1978).
[20] G. Barreau, H. G. Börner, T. von Egidy, and R. W. Hoff, Z. Phys. A **308**, 209 (1982).
[21] D. D. Warner, W. F. Davidson, W. Gelletly, J. Phys. G **5**, 1723 (1979).
[22] M. L. Stelts and R. E. Chrien, Nucl. Instrum. Methods **155**, 253 (1978).
[23] R. R. Spencer, J. A. Harvey, N. W. Hill, and L. W. Larson, Nucl. Sci. Eng. **96**, 318 (1987).
[24] G. Alaga, K. Alder, A. Bohr, and B. R. Mottelson, Mat. Fys. Medd. K. Dan. Vidensk. Selsk. **29**, (1955).
[25] D. H. White, R. E. Birkett, and T. Thompson, Nucl. Instrum. Methods **77**, 261 (1969).
[26] A. H. Wapstra and K. Bos, At. Data Nucl. Data Tables **19**, 215 (1977).
[27] F. A. Gareev, S. P. Ivanova, L. A. Malov, and V. G. Soloviev,

Nucl. Phys. **A171**, 134 (1971).
[28] T. H. Braid, R. R. Chasman, J. R. Erskine, and A. M. Friedman, Phys. Rev. C **4**, 247 (1971).
[29] R. R. Chasman, I. Ahmad, A. M. Friedman, and J. R. Erskine, Rev. Mod. Phys. **49**, 833 (1977).
[30] T. von Egidy, J. Almeida, G. Barreau, H. G. Börner, W. F. Davidson, R. W. Hoff, P. Jeuch, K. Schreckenbach, and D. H. White, Phys. Lett. **81B**, 281 (1979).
[31] J. Libert, M. Meyer, and P. Quentin, Phys. Rev. C **25**, 586 (1982).